




Case Studies of Rock Bursts Under Complicated Geological Conditions During Multi-seam Mining at a Depth of 800 m

Tong-bin Zhao^{1,2} · Wei-yao Guo^{1,2}  · Yun-liang Tan^{1,2} · Yan-chun Yin^{1,2} · Lai-sheng Cai³ · Jun-feng Pan⁴

Received: 7 October 2017 / Accepted: 19 January 2018 / Published online: 1 February 2018
© Springer-Verlag GmbH Austria, part of Springer Nature 2018

Abstract

A serious rock burst (“4.19” event) occurred on 19 April 2016 in the No. 4 working face of the No. 10 coal seam in Da’anshan Coal Mine, Jingxi Coalfield. According to the China National Seismological Network, a 2.7 magnitude earthquake was simultaneously recorded in this area. The “4.19” event resulted in damage to the entire longwall face and two gateways that were 105 m in long. In addition, several precursor bursts and mine earthquakes had occurred between October 2014 and April 2016 in the two uphill roadways and the No. 4 working face. In this paper, the engineering geological characteristics and in situ stress field are provided, and then the rock burst distributions are introduced. Next, the temporal and spatial characteristics, geological and mining conditions, and other related essential information are reviewed in detail. The available evidence and possible explanations for the rock burst mechanisms are also presented and discussed. Based on the description and analysis of these bursts, a detailed classification system of rock burst mechanisms is established. According to the main causes and different disturbance stresses (i.e., high/low disturbance stresses and far-field/near-field high disturbance stresses), there are a total of nine types of rock bursts. Thus, some guidelines for controlling or mitigating different types of rock bursts are provided. These experiences and strategies not only provide an essential reference for understanding the different rock burst mechanisms, but also build a critical foundation for selecting mitigation measures and optimizing the related technical parameters during mining or tunnelling under similar conditions.

Keywords Rock burst · Coal burst · Geology · Multi-seam mining · Mechanism · Mitigation

1 Introduction

A rock burst is a common dynamic disaster that is often accompanied by a sudden or violent ejection of coal or rock during the exploitation of underground resources. Rock bursts often occur in a complex way under special conditions, and sometimes without warning signs (Kaiser and Cai 2012; Feng et al. 2016; Zhao et al. 2017a, b). Such failure characteristics pose a great threat to the safety and efficiency of mining or tunnelling, and despite decades of studies, some aspects still need to be improved, especially case histories of rock bursts are not enough.

It is, however, generally acknowledged that the occurrence frequency of rock burst is not only related to intrinsic properties of coal or rock, such as stiffness, strength, bursting energy, elastic strain energy and dynamic failure duration (Cai et al. 2016; Kidybinski 1981; Lee et al. 2004; Singh 1988; Tan et al. 2016; Ning et al. 2017b), but also closely related to high stress concentration and disturbance stress. Both the high stress concentration and the disturbance

✉ Wei-yao Guo
363216782@qq.com

✉ Yun-liang Tan
yunliangtan@163.com

¹ State Key Laboratory of Mining Disaster Prevention and Control Co-founded by Shandong Province and the Ministry of Science and Technology, Shandong University of Science and Technology, Qingdao 266590, China

² College of Mining and Safety Engineering, Shandong University of Science and Technology, Qingdao 266590, China

³ Beijing Haohua Energy Resource Co., Ltd., Beijing 102304, China

⁴ Coal Mining and Designing Branch, Coal Research Institute China, Beijing 100013, China

stress include two aspects based on the causing reasons. For high stress concentration, one is high in situ stress caused by great mining depth, folds, faults and tectonic areas with facies change (Brauner 1994; Peng 2008; Whyatt and Varley 2009; Wang et al. 2012a, b; Huang et al. 2017; Feng et al. 2015b, c), and the second is high mining-induced stress controlled by mining engineering conditions, such as coal pillars, goaf, island working faces (i.e., a body of coal surrounded by previously mined faces), mining layout and multi-seam mining (Corkum and Board 2016; Li et al. 2016; Yu et al. 2016; Tan et al. 2015, 2017; Ning et al. 2017a; Zhang et al. 2018). While for disturbance stress (i.e., sudden stress perturbation), one is low disturbance stress induced by blasting, drilling, driving, coal cutting and other mining activities (He et al. 2012; Yan et al. 2015), and the second is high disturbance stress induced by hard roof fracturing and mine earthquake (Lu et al. 2015, 2016). Scholars and researchers have done lots of significant work on the causing reasons of rock bursts.

Regarding the aspects that cause high in situ stress and high mining-induced stress, scholars have studied rock bursts induced by various geological structures, coal pillars, island working faces, multi-seam mining, etc. For geological structures, Tan (1990) and Zhang et al. (2012) concluded that rock burst occurrences are closely related to folds. Wang et al. (2012a, b) analysed the mechanisms of coal bursts induced by geological structures, such as faults, folds and tectonic areas with facies changes. Wang and Zhang (2008), and Gu et al. (2015) obtained the stress distribution rule of syncline and anticline cores using numerical simulation. By using a numerical simulation and microseismic monitoring, Zhang (2015) and He et al. (2011) directly and indirectly proved that the core of a synclinal fold has a high in situ stress concentration, respectively. Li et al. (2008) and Jiang et al. (2013a, b) used mechanical analysis and numerical simulation to research the rules of rock bursts caused by faults and found that the risk of a fault slip rock burst is higher when the longwall face advances from the footwall to the fault itself rather than from the hanging wall to the fault. Zhou et al. (2015) and Meng et al. (2016, 2017) investigated methods for predicting rock bursts induced by the shear failure of structural planes in the deeply buried hard rock tunnels through various shear tests. Sainoki and Mitri (2014, 2016) established a dynamic model of fault slip and studied the dynamic behaviour of mining-induced fault slip through numerical simulation. Cai et al. (2014) studied the mechanical genesis of the Yima thrust nappe structure using a theoretical method. Iannacchione and Zelanko (1995), and Maleki et al. (2011) found that seam rolling and pitching also contribute to the heightened risk of a rock burst. Sun (2003) and Zhao et al. (2016) obtained the in situ stress distribution law in a region of variable coal thickness and studied the rock burst mechanism, respectively. Zhai et al. (2016)

concluded that the variation in the coal seam thickness significantly controls rock bursts based on case studies. For coal pillars, island working faces and multi-seam mining, Haramy and Kneisley (1990), and Li et al. (2015) confirmed that the yield pillars can effectively mitigate coal pillar bursts. Singh et al. (2011) found that mining-induced stress during a pillar extraction may vary with the site specific geological conditions. Cording et al. (2015) presented a design criterion for evaluating the overall stability of coal pillars. Yu et al. (2016) summarized in detail the factors affecting coal pillar stability and conducted stress and deformation monitoring to evaluate the performance of coal pillars. Li et al. (2016) presented a method to predict rock bursts in areas of likely occurrence on an island working face. Jiang et al. (2012) proposed an integrated approach for field tests and numerical investigations to assess the risk of rock bursts during stoping an island working face. Zhang et al. (2016) provided a width design method for gobs and isolated coal pillars based on overall burst instability prevention in coal mines. Feng et al. (2015a) set up a calculation model of abutment pressure and established a method for evaluating rock burst hazards for island working faces. Suchowerska et al. (2013) and Qu et al. (2015) demonstrated that the rock strata between coal seams experienced complicated deformation and failure processes during multi-seam mining. Guo et al. (2012) and Si et al. (2015) proved that the mining pressure of a longwall face and gateways behaves intensively under multi-seam mining conditions, which caused dynamic disasters. Jiang et al. (2011) analysed the mechanism of a load transfer between coal pillars with different widths under multi-seam mining conditions. Tan et al. (2017) preliminarily established a relationship between the increased height of failure zones after multi-seam mining with coal seam spacing, face size and lithology.

Many studies of disturbance stress have focused on hard roof fracturing because it is one of the main causes of rock bursts, whereas the other factors are mostly inducing factors. For studies of the roof fracturing, Jiang (2006) suggested that the spatial structure of strata can be divided into four types, which include θ -shaped, O-shaped, S-shaped and C-shaped structures. Tan et al. (2011) investigated the rock burst and acoustic emission (AE) pattern induced by three types of roof structures, including a brittle-thick-hard roof, flexible-thick-hard roof and fault activation. Zhao et al. (2012) and Jiang et al. (2013a, b) concluded that the seismic activity caused by hard roof failure can easily lead to a rock burst based on the analysis of microseismic data from two working faces. Lu et al. (2015, 2016) revealed the multi-parameter precursory characteristics and source distribution evolution rules pre and post-rock burst based on two rock burst hazards induced by hard roof caving. For other disturbance stresses, Xie and Li (2004) confirmed that blasting disturbance is not only a significant factor for rock burst

control, but also an important triggering factor for rock burst occurrence. Wang and Huang (1998), and Yan et al. (2015) proved that blasting disturbance has an important influence on the intensity and scale of rock bursts. He et al. (2012) found that the dynamic sources of blasting or coal cutting are the main inducing factors by analysing the rock bursts occurring in Taoshan Coal Mine. Ji et al. (2013) found that excavation methods influence the mechanical response of the surrounding rock through laboratory and field tests.

As a consequence of the above research and in addition to the intrinsic bursting proneness of coal or rock, the main aspects that cause high stress concentration and disturbance stress have been determined, and the meaningful results provide a good reference for understanding the mechanisms of rock burst induced by various factors. Despite the essential and valuable nature of case histories and studies, studies of rock bursts in multi-seam mining with complicated geological conditions are quite rare. Fortunately, Jingxi Coalfield is known as “China’s Geological Encyclopaedia” has very complicated geological conditions. One of its representations, Da’anshan Coal Mine, has witnessed more than twenty rock bursts/mine earthquakes between October 2014 and April 2016. This mine is rich in geological structures where multi-seam mining and mining at great depths occurred. The term “mine earthquake” in this manuscript refers to a seismic event with ground surface vibration. In particular, on 19 April 2016, a serious rock burst (“4.19” event) occurred in the No. 4 working face of the No. 10 coal seam. Simultaneously, a 2.7 magnitude earthquake was reported according to the China National Seismological Network, as shown in Fig. 1. There is no doubt that the analysis, summary and study of these rock bursts can build a critical foundation for the understanding, prediction, early warning and prevention of rock bursts in these types of mines or other underground engineering projects.

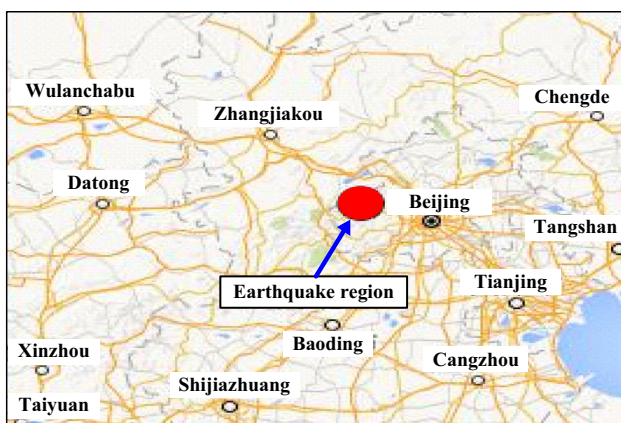


Fig. 1 Earthquake region recorded by China National Seismological Network on 19 April 2016

Therefore, three typical areas where rock bursts frequently occur were selected for this research in Da’anshan Coal Mine. First, we provide the engineering geological characteristics and in situ stress field, and introduce the rock burst distributions. Second, the temporal and spatial characteristics, geological and mining conditions, and other related information are reviewed in detail. Third, the available evidence and possible causes of rock bursts are presented and discussed. Finally, a detailed classification system of rock burst mechanisms is established, and some guidelines for controlling or mitigating the different types of rock bursts are provided.

2 Engineering Geological Characteristics and the In Situ Stress Field

2.1 Overview of Da’anshan Coal Mine

Da’anshan Coal Mine is located in Jingxi Coalfield, as shown in Fig. 2 (Wang et al. 2017). A previous published paper (Guo et al. 2017b) introduced an overview of Jingxi Coalfield, and thus, this section only presents an overview of Da’anshan Coal Mine. As seen in Fig. 2, Da’anshan Coal Mine is located west of the Tiaojishan-Miaoanling syncline with a length of 9 km in the strike direction and a width of 2–4 km in the dip direction. The mineable area is 25.5 km². The most common structures are folds accompanied by fault structures, which show a series of secondary anticlines or synclines. These anticlines are mostly in a closed state, whereas the synclines are in a broad and gentle state. Steep coal seams often show the reverse phenomena, and gentle inclined coal seams are located near/in the axial part of the Baicaotai overturned syncline. Thus, the development and excavation of coal in Da’anshan Coal Mine is primarily located near/in the axial part of the Baicaotai overturned syncline, as shown in Fig. 3. (Figure 3 mainly reveals the geological structures of the research area.) These complicated geological conditions induce the formation of tectonic areas with facies change, i.e., changes of coal seam thickness, coal seam dip angle, coal quality and coal seam overburden thickness, as shown in Fig. 4. Such complicated geological conditions not only lead to difficulties in coal production but also provide conditions for a rock burst occurrence.

Da’anshan Coal Mine has approximately 10 mineable coal seams, and the main mining coal seams three years ago from the bottom to top were the No. 5, 7, 9, 10, 13 and 14 coal seams. Recently, the main mining coal seams are the No. 5, 9 and 10 coal seams. Thus, when stoping the No. 10 coal seam of +400 Level, a multi-seam mining condition forms due to the left goaf and coal pillars in the No. 13 and 14 coal seams above it, which is illustrated in Fig. 3b.

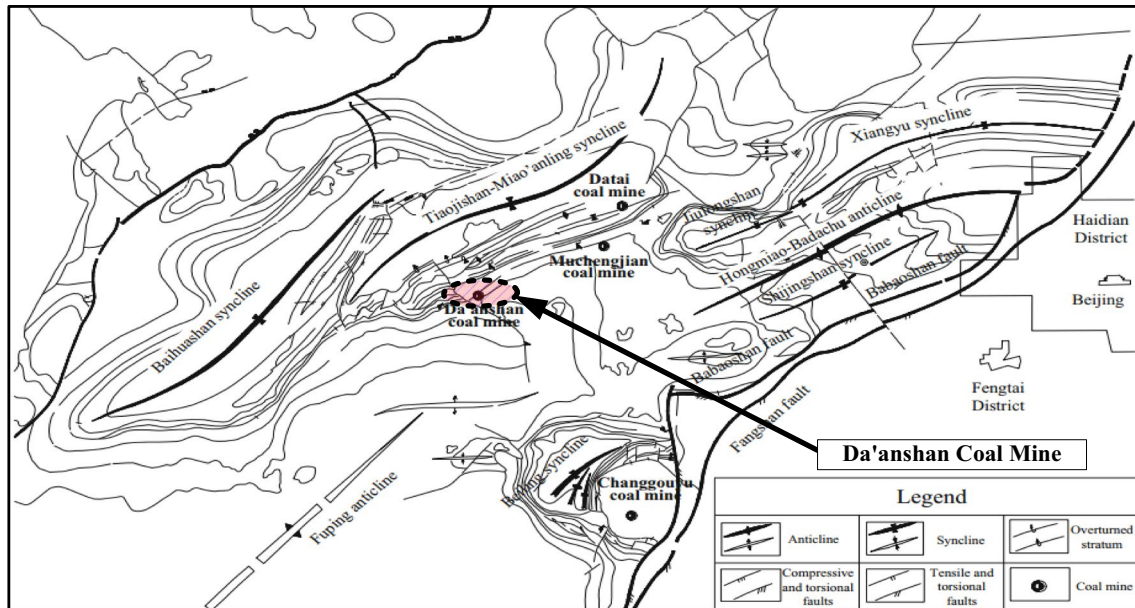


Fig. 2 Sketch map of geological structures in Jingxi Coalfield (Wang et al. 2017)

Figure 3b also reveals that the No. 10 coal seam is located between the south axial and the north axial of the Baicaotai overturned syncline and that the maximum mining depth reaches more than 1000 m. In addition to the complicated geological conditions, the multi-seam mining condition might also contribute to the high frequency of rock bursts in the No. 10 coal seam. Longwall technology was adopted in the research area.

2.2 Engineering Geological Conditions of the No. 10 Coal Seam

The No. 10 coal seam is 70° – 110° in the strike direction and 340° – 20° in the dip direction. The dip angle varies from 11° to 28° , and the average value is 19° . The formation and thickness of the coal seam that is close to the two synclinal axes of the Baicaotai overturned syncline vary greatly. Small faults with displacements of less than 2 m and joint fissures are richly developed under the influences of tectonic stress and gravity. These small faults are mostly normal faults. The arrangement of the working faces in the No. 10 coal seam of +400 Level is illustrated in Fig. 3a. The research area mainly includes four working faces, which include the No. 3, No. 4, W-No. 1 and E-No. 1 working faces.

The exploratory boreholes reveal that the No. 10 coal seam includes two seams, i.e., No. 10_{up} and No. 10_{down} coal seams. The thickness of the No. 10_{up} coal seam varies from 0.19 to 3.60 m with an average value of 1.82 m; the thickness of the No. 10_{down} coal seam varies from 0.38 to 3.23 m with an average value of 2.20 m. The distance between the No. 10_{up} and the No. 10_{down} coal seams is 0–3.78 m, and

there are merge phenomena in some regions. Figure 5 illustrates the lithological characteristics in detail. The main roof of the No. 10 coal seam includes hard fine sandstone and siltstone with a thickness of 30–50 m. In addition, the distance between the No. 14 and 13 coal seams is 46–53 m, with an average value of 50 m; the distance between the No. 13 and 10 coal seams is 62–116 m, with an average value of 90 m; the distance between the No. 10 and 9 coal seams is 23–43 m, with an average value of 38 m. In addition, the mining directions of the different working faces in the No. 13 and No. 14 coal seams were varied, which also leads to the complicated geological conditions.

The widths of the gate and the uphill roadway were 4.0 m and the heights varied. The two types of support schemes are illustrated in Fig. 6. The support schemes contain one type of bolt, one type of cable and steel belts/nets installed below them. The bolt was 18 mm in diameter and 2.0 m in length. The row and line spacing of the bolts were 1.2 m and 1.0 m, respectively. Polyurethane anchor resin was used to fix the bolts, and the length of the resin was 1.0 m. A torsion of 100 N·m was applied to the nuts of the bolts. The cable was 17.8 mm in diameter and 5.0 m in length. The row and line spacing of the cables were 2.4 m and 2.0 m, respectively. The length of the resin was 1.5 m. The preload for the cables had two values, which were 150 kN in the roof and 60 kN in the sidewall.

2.3 In Situ Stress Field

High in situ stress plays an essential role in dynamic disasters in underground mining, especially when the maximum

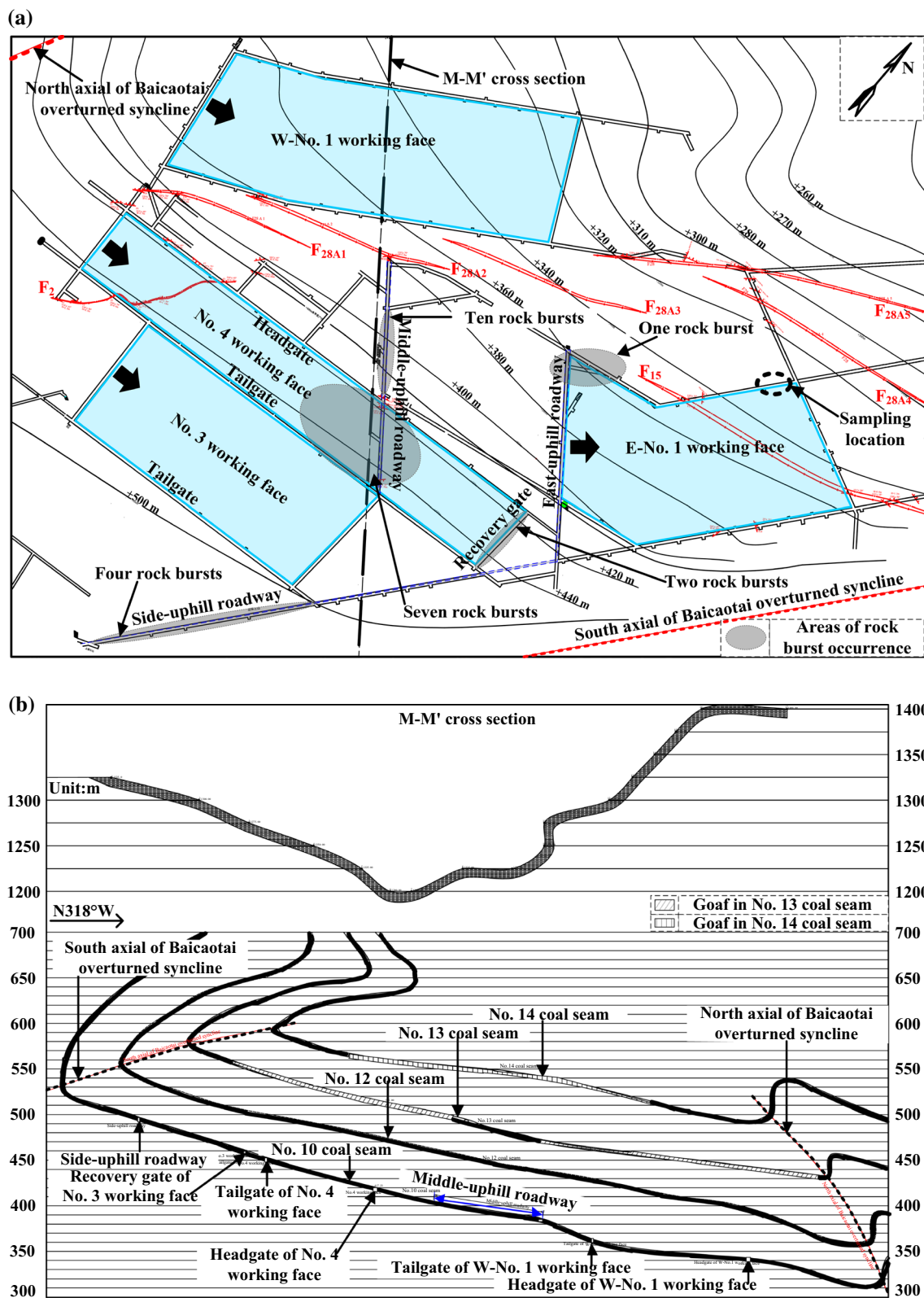


Fig. 3 Sketch of geological structures of the research area in Da'an Shan Coal Mine. **a** Part of the geological characteristics and the arrangement of working faces in the No. 10 coal seam of +400 Level **b** M-M' cross section

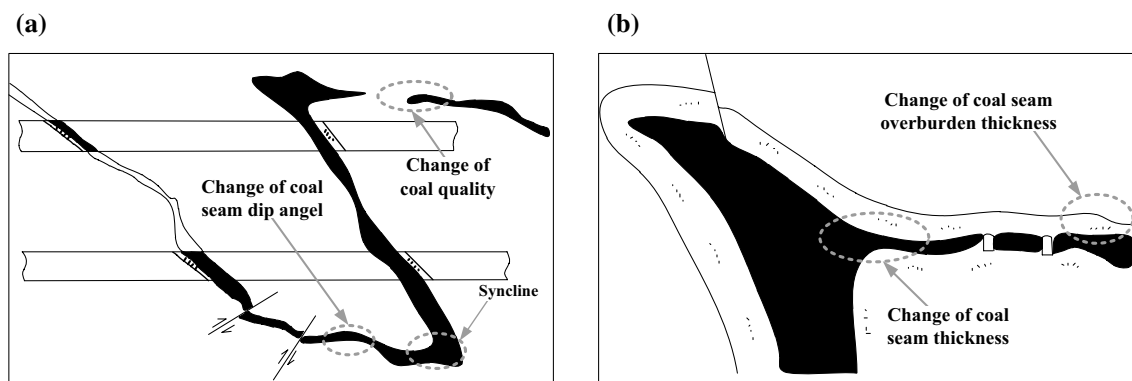


Fig. 4 Tectonic areas with facies change in Da'anshan Coal Mine. **a** Changes of coal seam dip angle and coal quality **b** changes of coal seam thickness and overburden thickness

mining depth reaches 1000 m in Da'anshan Coal Mine. Table 1 presents the results of the in situ stress measurements conducted at different depths in Da'anshan Coal Mine (Han et al. 2014). According to the field test, the primary characteristics of the geo-stress field are summarized as follows:

1. The maximum principal stress σ_1 increases with an increase in depth. For example, the maximum principal stress increases from 19.10 to 26.30 MPa with a growth of 37% when the buried depth increases from 465 to 672 m.
2. The dip angle of the maximum principal stress varies from -7.00° to 14.5° , which reveals that the direction of in situ stress is nearly horizontal. That is, the tectonic stress is the dominant stress field in Da'anshan Coal Mine.
3. The azimuth angle of the maximum principal stress is in the range of 213° – 252° , which indicates that the stress direction changes slightly.
4. The intermediate principal stress σ_2 varies from 12.20 to 13.50 MPa, which is almost equal to the gravity stress. The minimum principal stress σ_3 varies from 8.10 to 9.30 MPa in the horizontal direction with a dip angle of -9.00° to 15.00° except for the test result of 510 m depth. Generally, it could be concluded that the stress field of Da'anshan Coal Mine is in the plane of σ_1 and σ_3 .

Although the in situ stress in the No. 10 coal seam of +400 Level has not been tested, the great mining depth that varies from 700 to 1000 m means that this area has a higher in situ stress compared to the above test results. In addition, Wang et al. (2017) have proven that the in situ stress level in Jingxi Coalfield is greater than the average levels in Beijing area, North China and mainland China. Therefore, we can conclude that the research area has high in situ stress.

2.4 Coal Burst Liability

Coal burst liability (CBL) is an inherent property of coal that arises with an increase in the stored strain energy in the coal seam. Researchers have proposed various CBL indexes based on energy, stiffness, strength and failure duration. The standard CBL indexes widely used in China include the uniaxial compressive strength (R_C), elastic strain energy index (W_{ET}), bursting energy index (K_E) and dynamic failure duration (D_T). If the rock is weak, the energy and pressure will be released slowly, and the failure duration will last longer; but if the rock is hard, strong and brittle, the rock bursts will occur more easily, and the energy will release rapidly with a reduced failure time (Lee et al. 2004). The two indexes R_C and D_T are good choices for evaluating this intrinsic proneness. For the indexes W_{ET} and K_E , W_{ET} focuses on the capacity of the rock to absorb the external inputs of energy before it achieves peak strength, and K_E considers the accumulated elastic energy before peak strength and the released energy after the peak strength is achieved (Wang et al. 2017). These two indexes can determine the abilities of energy accumulation and energy release. Therefore, these four presented parameters are used as the Chinese standard. Table 2 lists the CBL classifications according to the Chinese standard (GB/T 25217.2-2010, 2010) as well as their calculations.

The CBL indexes were measured using coal samples obtained from the No. 10 coal seam of +400 Level. The sampling location is shown in Fig. 3a. Table 3 lists the test results of the No. 10_{up} and No. 10_{down} coal seams, and each index was obtained through the testing of five samples. For the No. 10_{up} coal seam, D_T , K_E , W_{ET} and R_C are 432 ms, 5.332, 2.632 and 27.279 MPa, respectively; for the No. 10_{down} coal seam, D_T , K_E , W_{ET} and R_C are 358 ms, 5.574, 1.754 and 23.770 MPa, respectively. The two indexes of K_E and R_C are larger than 5 and 14 MPa, respectively. Therefore, the No. 10 coal seam has a strong CBL based on the test results.

Fig. 5 Lithological characteristics of No. 10 coal seam

Rock strata	Thickness/m	Lithological descriptions
	30.00-50.00	Siltstone: Grey black, thin-medium thick layered rock, bedding development, medium hardness.
	1.20-2.80	No. 13 coal seam: Semidull coal, granular structure, good quality, soft.
	24.00-53.00	Siltstone: Grey black, thin-medium thick layered rock, bedding development, medium hardness.
	0.00-0.75	No. 12 coal seam: Semidull-semibright coal, stripped structure, step-like fracture, medium hardness, good quality.
	23.00-32.50	Siltstone: Grey black, thin-medium thick layered rock, bedding development, medium hardness.
	10.00-24.00	Fine sandstone: Dark grey, thick layered rock, containing quartz veins, tight cementation, high hardness.
	3.96-6.00	Siltstone: Grey black, thin-medium thick layered rock, bedding development, medium hardness.
	0.05-0.30	Carbonaceous siltstone: Grey black, thin layered rock, bedding development, broken seriously, easily caving.
	0.19-3.60 (No. 10 _{up})	No. 10 coal seam: Semidull-semibright coal, stripped structure, step-like fracture, medium hardness, good quality.
	0.00-3.78	
	0.38-3.23 (No. 10 _{down})	
	0.00-0.50	Carbonaceous siltstone: Grey black, thin layered rock, bedding development, broken seriously, easily caving.
	5.00-16.00	Siltstone: Grey black, thin-medium thick layered rock, bedding development, medium hardness.
	5.00-8.00	Fine siltstone: Black grey, medium thick-thick layered rock, high hardness.
	10.00-24.00	Fine sandstone: Dark grey, thick layered rock, containing quartz veins, tight cementation, high hardness.
	3.00-6.00	Siltstone: Grey black, thin-medium thick layered rock, bedding development, medium hardness.
	0.00-0.30	Carbonaceous siltstone: Grey black, thin layered rock, bedding development, broken seriously, easily caving.
	0.59-4.26 (No. 9 _{up})	No. 9 coal seam: Semidull coal, granular structure, medium hardness, good quality.
	0.00-1.30	
	0.91-2.81 (No. 9 _{down})	
	0.00-0.20	Carbonaceous siltstone: Grey black, thin layered rock, bedding development, broken seriously, easily caving.
	5.00-16.00	Siltstone: Grey black, thin-medium thick layered rock, bedding development, medium hardness.
	8.00-10.00	Siltstone: Black grey, medium thick-thick layered rock, high hardness.

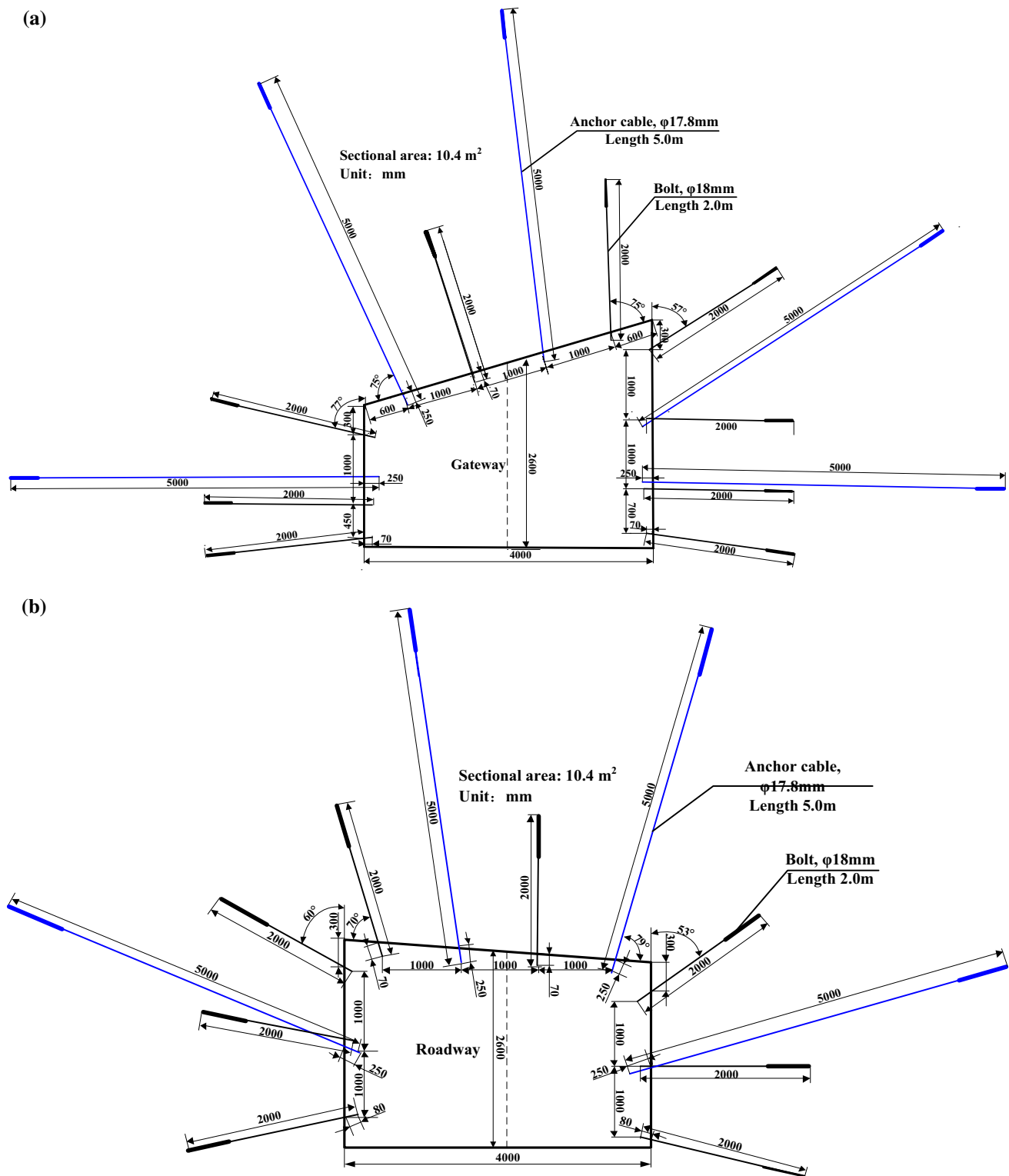


Fig. 6 Support schemes of gateway and uphill roadway. **a** Gateway **b** uphill roadway

3 Rock Burst Distributions

In addition to the arrangement of the working faces in the No. 10 coal seam of +400 Level, the main burst areas are

marked by the light grey oval in Fig. 3a. From Fig. 3a, it can be seen that these events occurred in five areas. There are twenty-four rock bursts, which include four in the side-uphill roadway, ten in the middle-uphill roadway, seven in

Table 1 Test results of in situ stress in Da'anshan Coal Mine (Han et al. 2014)

Depth/m	Maximum principal stress (σ_1)			Intermediate principal stress (σ_2)			Minimum principal stress (σ_3)		
	Value/MPa	Azimuth angle/ $^\circ$	Dip angle/ $^\circ$	Value/MPa	Azimuth angle/ $^\circ$	Dip angle/ $^\circ$	Value/MPa	Azimuth angle/ $^\circ$	Dip angle/ $^\circ$
465	19.10	232.00	12.00	12.40	358.00	70	8.10	139.00	15.00
510	20.50	252.00	- 7.00	12.20	344.00	- 5	9.30	109.00	- 80.00
580	22.60	213.00	1.00	12.60	302.00	- 80	9.20	122.00	- 9.00
672	26.30	244.00	14.50	13.50	301.00	- 64	8.60	159.00	- 20.00

Table 2 Index values of CBL classification in the Chinese standard (GB/T 25217.2-2010 2010)

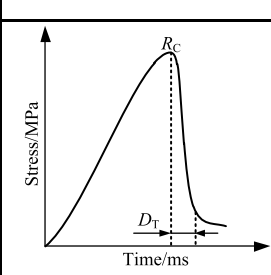
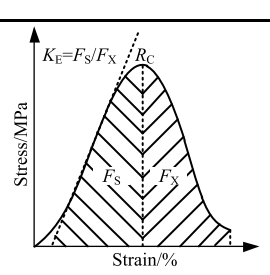
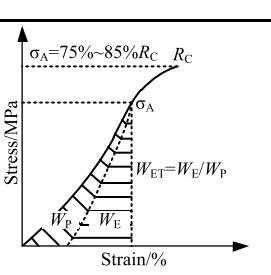
Coal burst liability indexes	D_T /ms	K_E	W_{ET}	R_C /MPa
Schematic drawing of calculation				
Test method	Uniaxial compression test			
Strong burst	≤ 50	≥ 5.0	≥ 5.0	≥ 14
Weak burst	50~500	5.0~1.5	5.0~1.5	14~7
None burst	> 500	< 1.5	< 1.5	< 7

Table 3 Test results of CBL of No. 10 coal seam

CBL index	D_T /ms	K_E	W_{ET}	R_C /MPa	Classification
No. 10 _{up} coal seam	372–491	4.354–6.434	1.852–3.089	25.146–31.223	Strong burst
Average value	432	5.332	2.632	27.279	
No. 10 _{down} coal seam	304–459	4.633–6.441	1.544–2.244	20.153–26.987	Strong burst
Average value	358	5.574	1.754	23.770	

the No. 4 working face, two in the recovery gate and one in the east-uphill roadway. Of note is that some of these bursts were accompanied by mine earthquakes. Specifically, fourteen rock bursts occurred in the side-uphill and middle-uphill roadways after 6–16 months of roadway excavation; seven rock bursts occurred in the No. 4 working face during the stopping process; and three rock bursts occurred in the recovery gate and east-uphill roadway during the tunneling process. A new phenomenon is that creep-induced rock bursts account for nearly 54% of all rock bursts, but their damage was lesser serious compared with the bursts occurring during the stopping process. Above all, these rock bursts are mostly concentrated in three areas, i.e., the side-uphill roadway, the middle-uphill roadway and the No. 4 working face. Therefore, in this paper, these three areas are selected for further research. In the next section, the temporal and spatial characteristics of each rock burst occurring in the selected research areas are described in detail. In addition,

the related engineering and geological characteristics are investigated carefully, and possible explanations for the observed results are discussed.

4 Description and Analysis of Rock Bursts

4.1 The Side-Uphill Roadway

Figure 7 presents the region of rock burst occurrence and the related mining and geological characteristics of the side-uphill roadway. From 10 October 2014 to 13 February 2015, four rock bursts occurred in the side-uphill roadway without the occurrence of mine earthquakes or mining disturbances. Among these rock bursts, the burst that occurred on 10 October 2014 (“10.10” event) influenced the gateway over 150 m in length with slight damage, which caused coal cinder drop and 0–40 mm floor heave. The other three bursts only

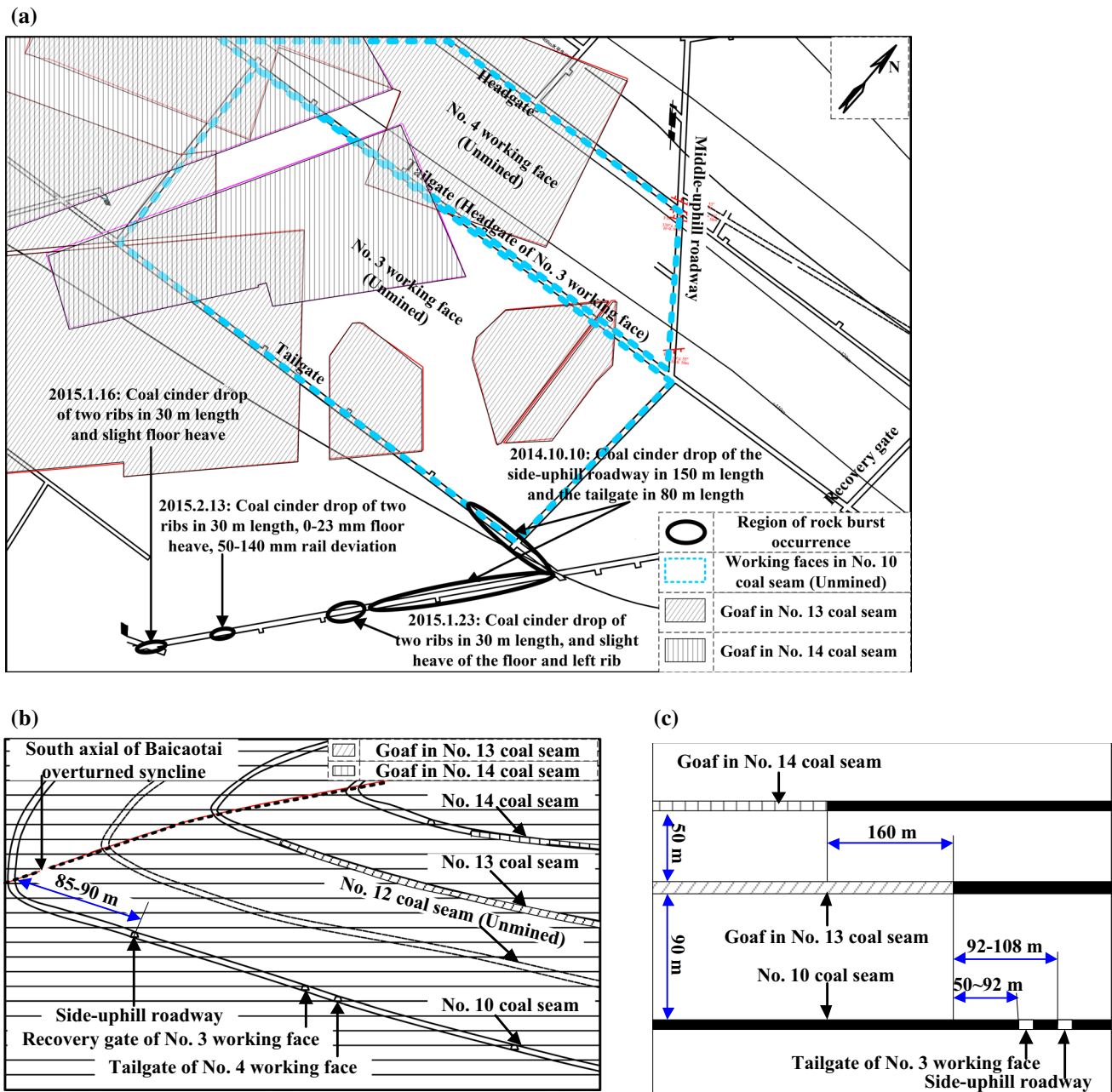


Fig. 7 Region of rock burst occurrence, and the related mining and geological characteristics in the side-uphill roadway. **a** Region of rock burst occurrence and mining characteristics **b** cross section of coal

seam group **c** sketch of positional relationship between No. 10, 13 and 14 coal seams

influenced the gateway over 30 m in length, which caused coal cinder drop and 0–23 mm floor heave. In addition, the side-uphill roadway had been excavated for more than 6 months, i.e., these bursts are creep-induced rock bursts.

The mining depth was 700–800 m, and the distance between the side-uphill roadway and the axial of the Baicaotai overturned syncline was only 85–90 m, which is shown in Fig. 7a, b. Many studies have proven that the core of the synclinal fold is a high in situ stress concentration area (He

et al. 2011; Gu et al. 2015; Zhang et al. 2012; Zhang 2015). Thus, considering the mining depth and syncline, the upside roadway obviously experienced high tectonic stress. In addition, the coal pillars left in the No. 13 and No. 14 coal seams might also contribute to the stress concentration but are not the main factor due to the long horizontal distance between the goaf edge and the roadway, which is shown in Fig. 7c. The side-uphill roadway belongs to a high static stress concentration area (note: the mine workers also reported that

when the side-uphill roadway was excavated, the roadway experienced large deformation and high pressure). Above all, it could be concluded that the four creep-induced rock bursts are closely related to the change of coal/rock structure and the high static stress.

Fortunately, practical experiences reveal that creep-induced rock bursts induced by tectonic stress could be controlled or mitigated. For example, no mitigation methods of rock bursts were taken before the “10.10” event, and only a large-diameter drilling method was used after this event. The borehole length was 15 m, borehole space was 5 m, borehole diameter was 110 mm, and one row of boreholes was located in the middle of each coal wall. However, three weaker rock bursts still occurred due to an insufficient stress relief after the “10.10” event. Thus, the borehole space for large-diameter drilling was optimized into 1 m, and the water infusion method was added. The borehole length for water infusion was 15 m, borehole space was 5 m, borehole diameter was 76 mm, water infusion pressure was 16 MPa, and one row of boreholes was located in the middle of each coal wall. By adopting this mitigation strategy, no further bursts occurred in the side-uphill roadway.

4.2 The Middle-Uphill Roadway

Figures 8 and 9 show the region of rock burst occurrence between 18 November 2014 and 17 July 2015, and between 21 October 2015 and 29 February 2016 in the middle-uphill roadway, respectively. The related mining and geological

characteristics are also illustrated. Photographs of the damage from the two rock bursts that occurred on 17 July 2015, and 29 February 2016 are illustrated in Fig. 10. The mining depth of this area was 700–800 m. Before the presentation and analysis, we need to explain that these rock bursts also occurred after more than 6 months of roadway excavation. The damage and other information of the ten bursts are listed in Table 4.

4.2.1 Rock Bursts Occurring Between 18 November 2014 and 17 July 2015

As shown in Fig. 8, four rock bursts occurred without the occurrence of a mine earthquake near the headgate throat between 18 November 2014 and 17 July 2015. During the first two bursts, there were no mining disturbances; during the other two bursts, the longwall face of the No. 3 working face was more than 140 m away. That is, the mining disturbance slightly affected. Due to the great mining depth, tectonic areas with facies change and left coal pillars in the No. 13 coal seam, the burst region had an obvious high static stress concentration. In addition, the triangular area may also contribute to this. Thus, these bursts might also belong to creep-induced rock bursts, which are related to the high static stress. From Table 4, it can be seen that the damage from these four rock bursts was not serious.

Then, two mitigating methods were applied after these four bursts. One was the large-diameter drilling method used for destressing coal walls, and the other was the loosening

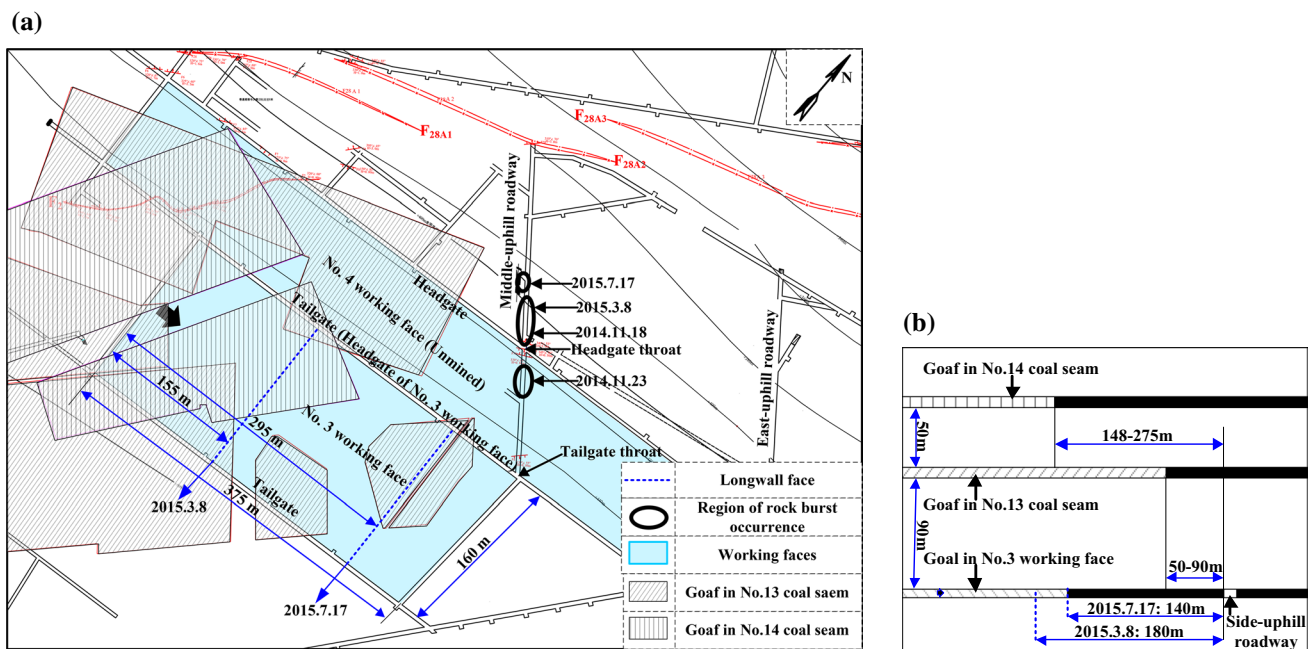


Fig. 8 Region of rock burst occurrence, and the related mining and geological characteristics in the middle-uphill roadway between 18 November 2014 and 17 July 2015. **a** Region of rock burst occurrence and mining characteristics **b** sketch of positional relationship between coal seams

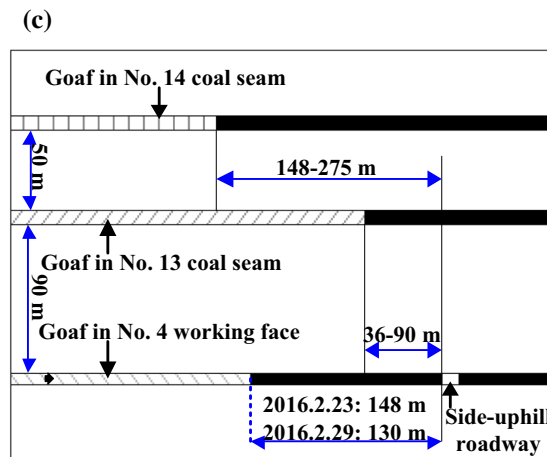
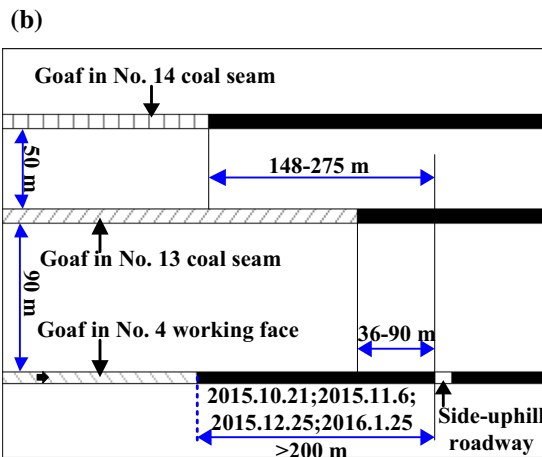
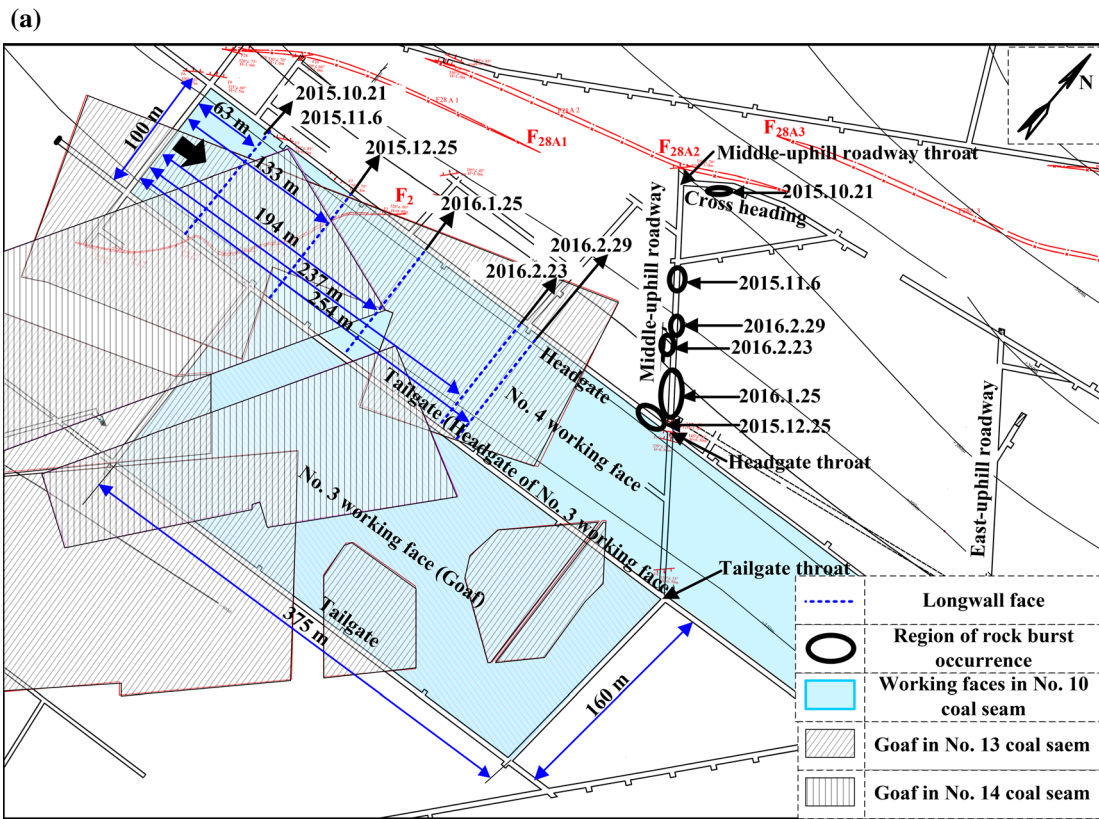


Fig. 9 Region of rock burst occurrence, and the related mining and geological characteristics in the middle-uphill roadway between 21 October 2015 and 29 February 2016. **a** Region of rock burst occur-

rence and mining characteristics **b–c** sketch of positional relationship between coal seams

blasting method used for destressing floors. For the large-diameter drilling, the borehole length was 15 m, borehole space was 1 m, borehole diameter was 110 mm, and one row was located in the middle of each coal wall; for the loosening blasting, a loosening pot-bottom area with 1–2 m depth was formed in the floor. However, it seems that the destressing degree was not enough, and another five rock bursts subsequently occurred in this area.

4.2.2 Rock Bursts Occurring Between 21 October 2015 and 29 February 2016

As shown in Fig. 9, six rock bursts occurred between 21 October 2015 and 29 February 2016. It is very interesting that the damage from these rock bursts was slight even though they were accompanied with mine earthquakes, which is shown in Table 4. Except for the rock burst that

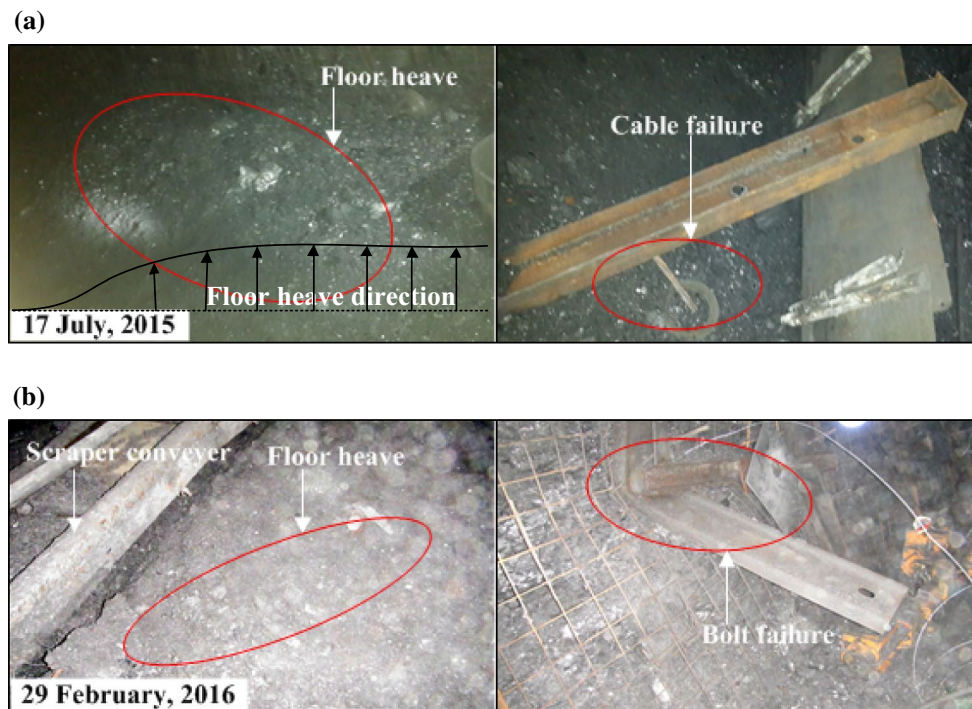


Fig. 10 Damage of the two rock bursts on 17 July 2015 and on 29 February 2016 in the middle-uphill roadway. **a** 17 July 2015 **b** 29 February 2016

Table 4 Damage characteristics of rock bursts in the middle-uphill roadway

Date	Damage characteristics	Mine earthquake
18 November 2014	The damage includes slight floor heave, and obvious scratches of bolt or cable trays	No
23 November 2014	Coal cinder drop of two coal walls	No
8 March, 2015	(1) The range of 10–50 m from headgate throat to the north mainly experienced coal cinder drop and floor heave. Specifically, the range of 10–30 m had rib heave and 100–400 mm floor heave; the range of 34–48 m had 100–300 mm floor heave. In addition, a fracture (100 mm width, 400 mm depth and 1.2 m length) also appeared in the position of 22 m (2) The range of 6–13 m from headgate throat to the east saw two fractures with length of 10 mm and 100 mm, respectively	No
17 July 2015	The range of 50–65 m from headgate throat to the north had 100 mm rib heave and 200 mm floor heave, causing failure of one cable	No
21 October, 2015	There were fractures near the F_{28A3} fault in the range of 23–27 m from middle-uphill roadway throat to the east, and the damage also included 100 mm floor heave and 200–300 mm right rib heave	Yes
6 November 2015	The range of 106–116 m from headgate throat to the north experienced 150 mm floor heave	Yes
25 December 2015	There were fractures in the floor from headgate throat to the west of 0–30 m, but no changes for the two coal walls	Yes
25 January 2016	The range of 10–30 m from headgate throat to the north experienced 100–200 mm floor heave, and failure of eight bolts and one cable	Yes
23 February 2016	The range of 55–65 m from headgate throat to the north saw 200–300 mm floor heave, failure of four bolts in the left rib, and ejection of one cable tray	Yes
29 February 2016	The range of 66–86 m from headgate throat to the north experienced 100–300 mm floor heave, and failure of two bolts	Yes

occurred on 21 October 2016 (“10.21” event) in the cross-heading, the other five occurred in the middle-uphill roadway.

There is no question that the “10.21” event had a close relation with the F_{28A2} fault, because the burst region was more than 200 m away from the longwall face of No. 4 working face, but it was located near the F_{28A2} fault. Based on the degree of damage, it seems that the mine earthquake might make little contribution and may just be an inducing factor. Although it is essential to know the source point for each mine earthquake, there was no microseismic (MS) monitoring system in Da’anshan Coal Mine before the “4.19” event. Fortunately, the KJ768 MS monitoring system was installed in the W-No. 1 working face after the “4.19” event, which could provide some supplementary information in this paper for analysing the occurrence mechanisms of these rock bursts (note: some of the MS monitoring information will be added in Sect. 5.2).

As mentioned in Sect. 4.2.1, the burst region in the middle-uphill roadway had high a static stress concentration. Although the five bursts occurring between 6 November 2015 and 29 February 2016 were accompanied by mine earthquakes, their damage was rather slight. This phenomenon again reflects that the mine earthquake was not the controlling factor. The longwall face of No. 4 working face was more than 200 m during the first three bursts and 130–148 m during the second two bursts. According to the original monitoring of the abutment pressure distribution, the burst region was still out of the influencing range. Overall, these

five bursts might also belong to creep-induced rock bursts, but were accompanied by far-field disturbance stress, i.e., mine earthquake.

During this period, the loosening blasting of the floor was completed twice, and another row of large-diameter boreholes was drilled. In addition to these two methods, water infusion was also added. For water infusion, the borehole length was 15 m, borehole space was 5 m, borehole diameter was 76 mm, water infusion pressure was 16 MPa, and one row of boreholes was located in the middle of each call wall. Hereafter, no more rock bursts again occurred in the middle-uphill roadway, and the later bursts mainly focused in the longwall face and the two gateways of No. 4 working face. These practical experiences reveal that the creep-induced rock bursts induced by the high static stress concentration could be controlled or mitigated.

4.3 The No. 4 Working Face

Figure 11 presents the region of rock bursts and related mining and geological characteristics between 23 March and 19 April 2016 in the No. 4 working face. These bursts all occurred during the stoping process, and most of them were accompanied by mine earthquakes. The damage description and other information for all nine events are listed in Table 5. Two of the events were mine earthquakes that occurred without any damage. This phenomenon again reveals that the mine earthquake might just be an inducing factor. Among the seven rock bursts, three led to serious damage, which

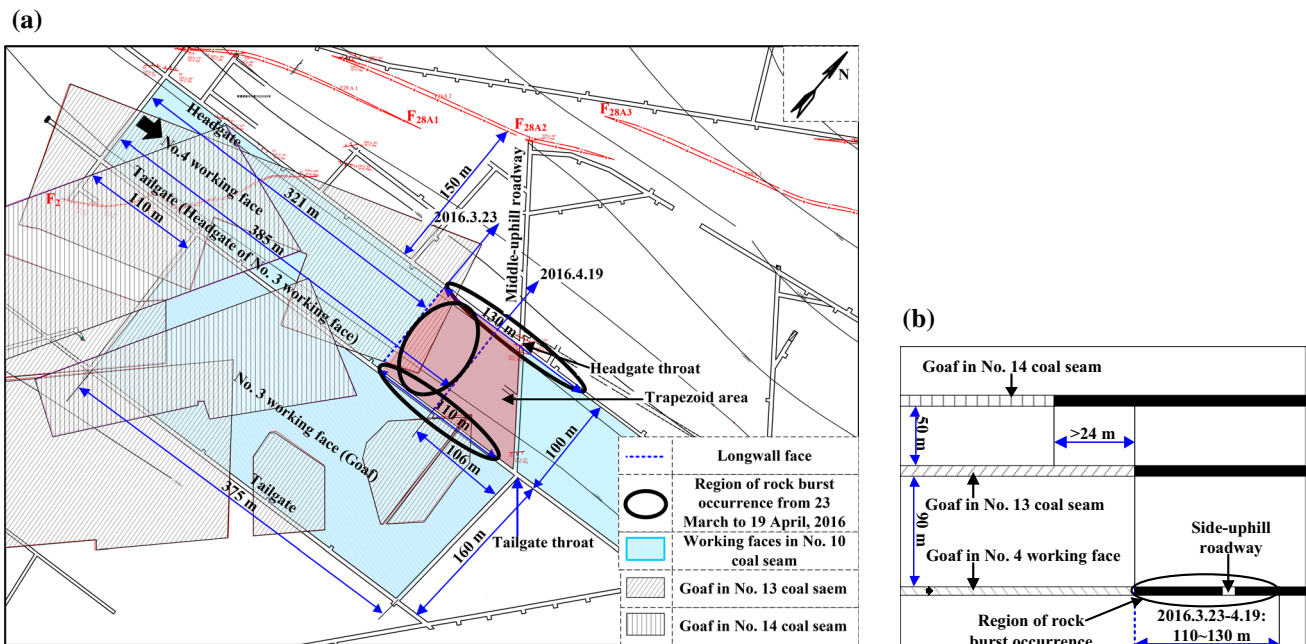


Fig. 11 Region of rock burst occurrence, and the related mining and geological characteristics in the No. 4 working face between 23 March 2016 and 19 April 2016. **a** Region of rock burst occurrence and mining characteristics **b** sketch of positional relationship between coal seams

Table 5 Damage characteristics of rock bursts in the No. 4 working face

Date	Damage characteristics	Mine earthquake
23 March 2016	The tailgate had a 200–300 mm floor heave in front of the longwall face 20–25 m, causing 200–300 mm displacement of the props	No
30 March 2016 (Morning)	No damage	Yes
30 March 2016 (Noon)	The headgate experienced 100–200 mm floor heave in front of the longwall face 3–23 m, and the left rib had a 100–150 mm displacement in front of 0–31 m and 50–57 m. At this time, the distance between the headgate and the middle–uphill roadway was 71 m	Yes
31 March 2016 (“3.31” event)	(1) The longwall face in the range of 0–15 m from up to down had a serious floor heave and slight rib spalling. The range of 61–96 m experienced serious rib spalling with the maximum value of 1000 mm, causing leakage of safety valve; the range of 82–84 m even saw a 50 mm displacement of No. 55–56 props and scraper conveyer (2) The affected range of tailgate is 0–85 m in front of the longwall face. Specifically, the range of 0–20 m had 500 mm floor heave; the range of 20–26 m had 200 mm floor heave and 300–500 mm rib displacement; the range of 26–49 m experienced 600–1000 mm floor heave, leading to the height of tailgate varied from 1.2 to 1.6 m; the range of 58–84 m saw 200–500 mm floor heave and 100–300 mm rib displacement, including broken of one hydraulic prop and one cable in the position of 73 m. In addition, the middle row of hydraulic props all had displacement	Yes
4 April 2016	The longwall face in the range of 14–34 m from up to down had slight rib spalling	Yes
6 April 2016	No damage	Yes
12 April 2016 (“4.12” event)	(1) The longwall face in the range of 0–16.5 m had rib spalling (2) The headgate in the range of 0–23 m from the longwall face to the east had 100–200 mm floor heave, and in the range of 14–45 m from headgate throat to the east experienced 300–500 mm floor heave and right rib spalling	Yes
17 April 2016	The middle–upper part of the longwall face had slight rib spalling	No
19 April 2016 (“4.19” event)	(1) The headgate had serious deformation in front of the longwall face 0–15 m, causing the bending of hydraulic props. The gateway’s height and width were only left 1.5 m and 1.3 m, respectively (2) The whole longwall face had rib spalling, especially in the range of 29–67.5 m from up to down, the serious rib spalling caused the close of supporting area. Meanwhile, the scraper conveyer was uplifted (3) The displacement of coal cutter caused the bending or even broken of hydraulic props in the range of 46.5–52.5 m (4) The tailgate experienced serious floor and rib heave in front of the longwall face 0–90 m. These hydraulic props closed to the left rib were pulled down, and four of them were broken. Especially in the range of 26–56 m, the serious floor and rib heave almost caused the close of the tailgate, while the ranges of 0–26 m and 56–90 m had 200–1000 mm floor heave and 200–600 mm left rib heave (5) The scraper and belt conveyers in the headgate could not function	Yes

occurred on 31 March (“3.31” event), 12 April (“4.12” event) and 19 April (“4.19” event). For the longwall face, the three bursts caused serious rib heave/spalling with a maximum displacement of 1000 mm and prop damage. For the two gateways, the events caused floor and rib heave/spalling with a maximum value of 1000 mm as well as prop damage and failure of bolts or cables. In some regions, the serious damage even led to the closing of the gateway or longwall face. Photographs of the damage from the three serious rock bursts are shown in Fig. 12.

The average mining depth of No. 4 working face was 810 m. The distance between the burst region and the F_{28A2} fault was more than 150 m. As shown in Sect. 2.2, the No. 10 coal seam contained parting bands, and its main roof was a hard fine sandstone and siltstone of 30–50 m in thickness. Many scholars have proven that hard roof fracturing could lead to high dynamic stress (Lu et al. 2015, 2016;

Zhao et al. 2012; Jiang et al. 2013a, b). Tectonic areas with facies change also existed in this working face. Moreover, the burst region was next to the goaf of No. 3 working face and was below the left coal pillars of the No. 13 coal seam. As shown in Fig. 11a, a trapezoid area with a high stress concentration superposed because of the high in situ stress and the high mining-induced stress was formed under the influences of different factors. Thus, this area had the potential to experience a high frequency of rock bursts, especially during the stoping process.

Large-diameter drilling and water infusion methods were both used for improving the stress conditions during the stoping process. For large-diameter drilling, the borehole length was 15 m, borehole space was 15 m, borehole diameter was 110 mm, and one row was located in the middle of each coal wall; for the water infusion, the borehole length was 15 m, borehole space was 5 m, borehole

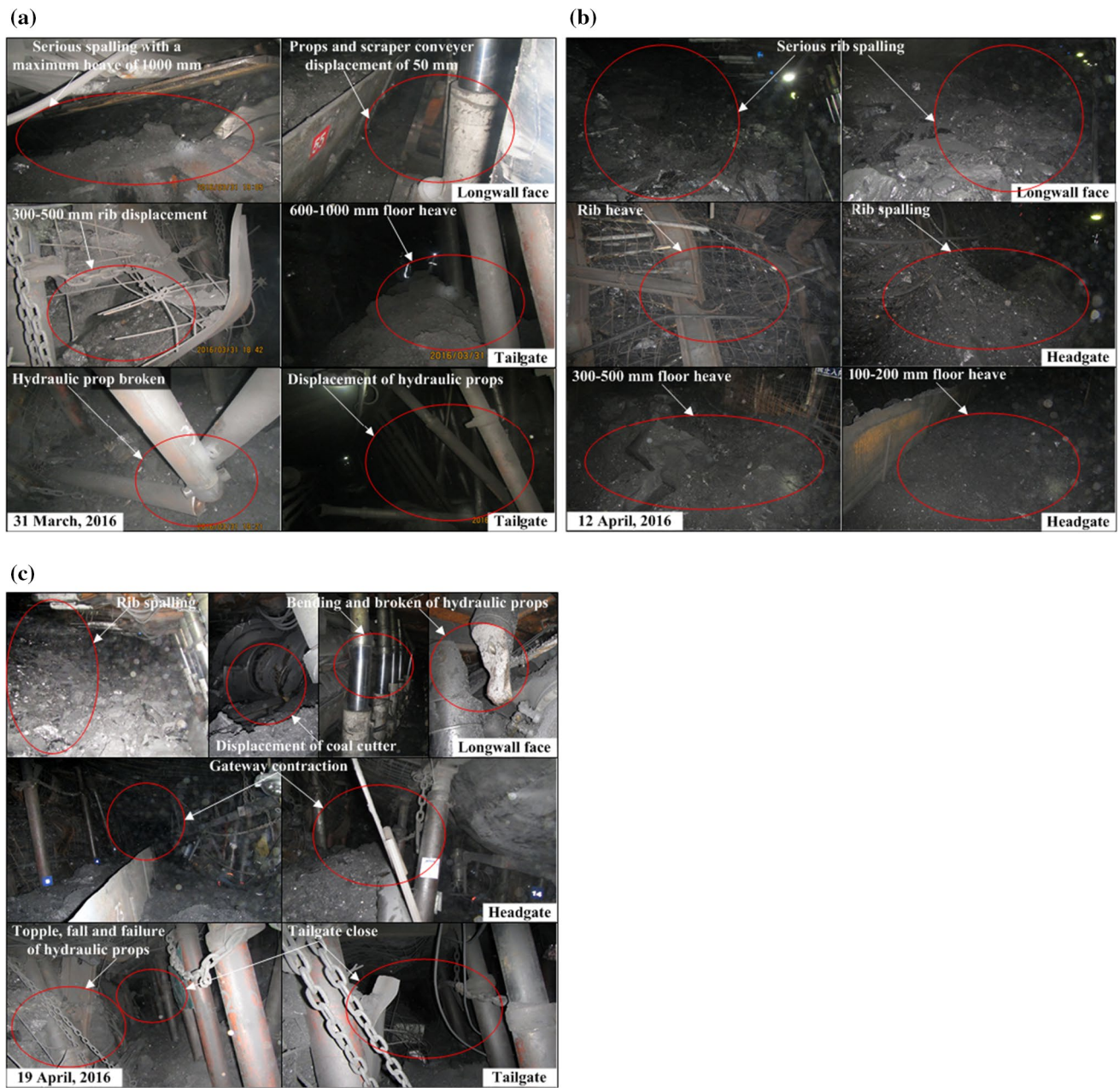


Fig. 12 Damage of the three rock bursts on 31 March, 12 April, and 19 April, respectively, in the No. 4 working face. **a** 31 March 2016 (“3.31” event) **b** 12 April 2016 (“4.12” event) **c** 19 April 2016 (“4.19” event)

diameter was 76 mm, water infusion was 16 MPa, and one row was located in the middle of each coal wall. The length of the water infusion was 0–80 m in front of the longwall face. Unfortunately, they only functioned well during the early stoping process below the goal of the No. 13 coal seam and failed below the coal pillars of the No. 13 coal seam. This phenomenon reveals that the coal pillars of the No. 13 coal seam had an essential contribution to the stress concentration and that the goaf led to stress relief.

In addition, the longwall face pressure and abutment pressure were monitored during the stoping process of the No. 4 working face. The monitoring scheme and equipment are shown in Fig. 13. The sensors (YHY60(A) mine pressure gauge) for monitoring the longwall pressure were located at intervals of 10 m, and the whole longwall face was monitored. The sensors (YHY60(C) mine pressure detector) for monitoring the abutment pressure were located at intervals of 5 m, and the monitoring length was 25 m in front of the longwall face. The two types of sensors used were made by

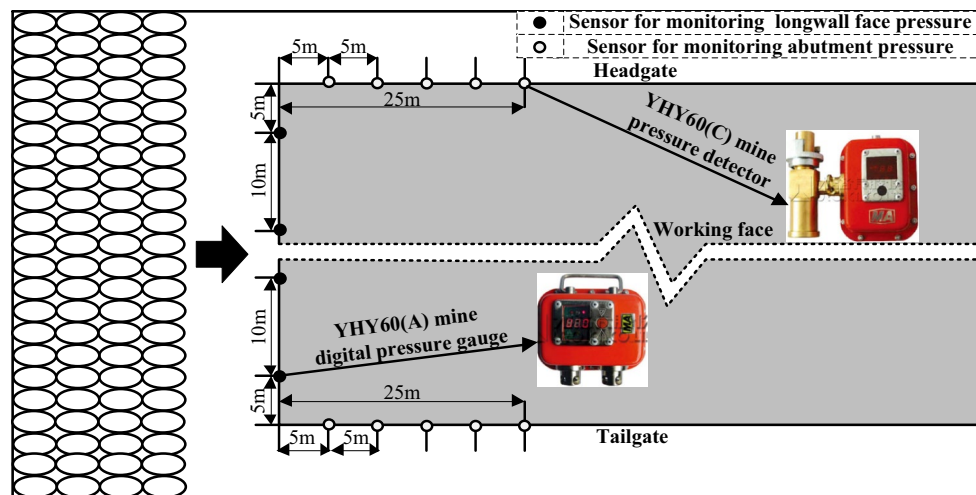


Fig. 13 Pressure monitoring scheme and equipment

Uroica Mining Security Engineering Co., LTD. The pressure values were recorded three times a day. The mean value was selected as the monitoring result for each time (note: the pressure monitoring information will be added in Sect. 5.2).

5 Discussion of the Rock Burst Mechanism and Mitigating Strategies

Guo et al. (2017b) proposed three types of rock burst mechanisms, i.e., “high in situ stress”, “high mining-induced stress” and “high in situ stress plus high mining-induced stress” rock bursts, which was based on the main cause for high stress concentrations, as illustrated in Fig. 14a. From the description and analysis in Sect. 4, all of the research areas had a high in situ stress due to the great mining depth and complicated geological conditions. Moreover, the middle-uphill roadway and No. 4 working face also had high mining-induced stress due to the influences of the goaf of the No. 3 working face and left coal pillars of the No. 13 coal seam. Therefore, the bursts in the side-uphill roadway could be classified as “high in situ stress” rock bursts, whereas in the middle-uphill and No. 4 working face, these could be classified as “high in situ stress plus high mining-induced” rock bursts. However, the above classification is rather rough, because many rock bursts are accompanied by different disturbance stresses. In particular, hard roof breaking is one of the main factors that cause rock bursts. Thus, this classification could be expressed more carefully.

From the above perspective, we could classify the disturbance stresses into low disturbance stress (i.e., blasting, drilling, driving and coal cutting) and high disturbance stress (i.e., hard roof fracturing and mine earthquake). Based on this point, rock burst mechanisms still have three major

groups, which includes I “high in situ stress plus low/high disturbance stress”, II “high mining-induced stress plus low/high disturbance stress”, and III “high in situ stress plus high mining-induced stress plus low/high disturbance stress” rock bursts, which are illustrated in Fig. 14b. Due to the high in situ stress, only rock burst types I and III exist in these research areas. The detailed analysis of these rock bursts in the No. 10 coal seam of +400 Level is as follows.

5.1 “High In Situ Stress Plus Low/High Disturbance Stress” Rock Bursts

These rock bursts in the side-uphill roadway occurred after 6 months of roadway excavation. During the occurrence period, there were no mining disturbances or mine earthquakes. The side-uphill roadway was mainly influenced by the great mining depth and geological structures. Thus, the bursts in the side-uphill roadway belong to the “high in situ stress plus low disturbance stress” rock burst. In other words, high in situ stress could lead to a creep-induced rock burst (note: the occurrence mechanism of creep-induced rock bursts still needs further extensive research). Fortunately, a “high in situ stress plus low disturbance stress” rock burst could be controlled or mitigated, which is shown in Sect. 4.1.

5.2 “High In Situ Stress Plus High Mining-Induced Stress Plus Low/High Disturbance Stress” Rock Bursts

Due to the great mining depth, the tectonic areas with facies change and the left coal pillars of the No. 13 coal seam, the middle-uphill roadway had high in situ stress and high mining-induced stress, but the disturbance stresses of these rock bursts were different. The first four rock bursts occurred

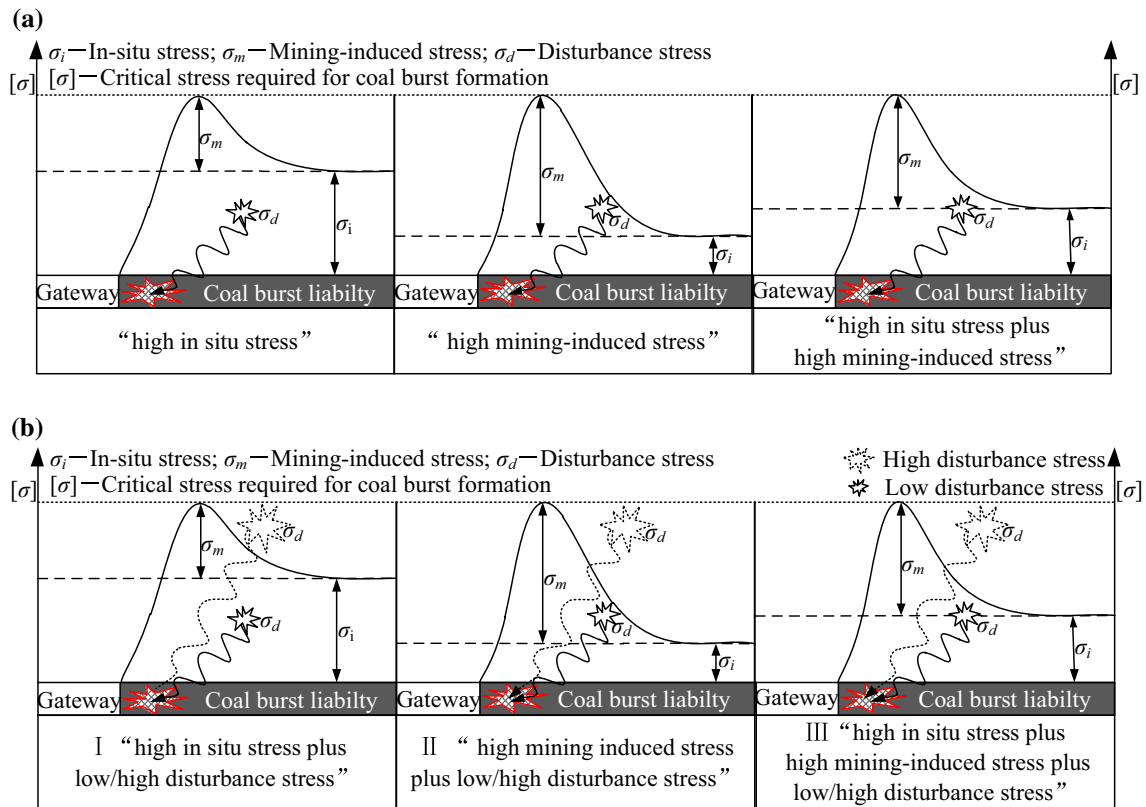


Fig. 14 Sketch of rock burst mechanisms. **a** Rock burst mechanisms without considering different disturbance stresses (Guo et al. 2017b) **b** rock burst mechanisms with different disturbance stresses

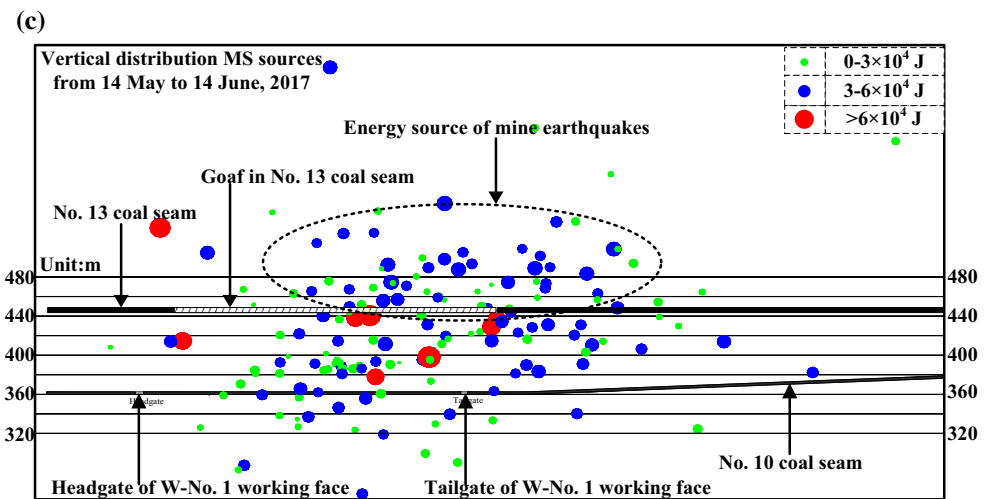
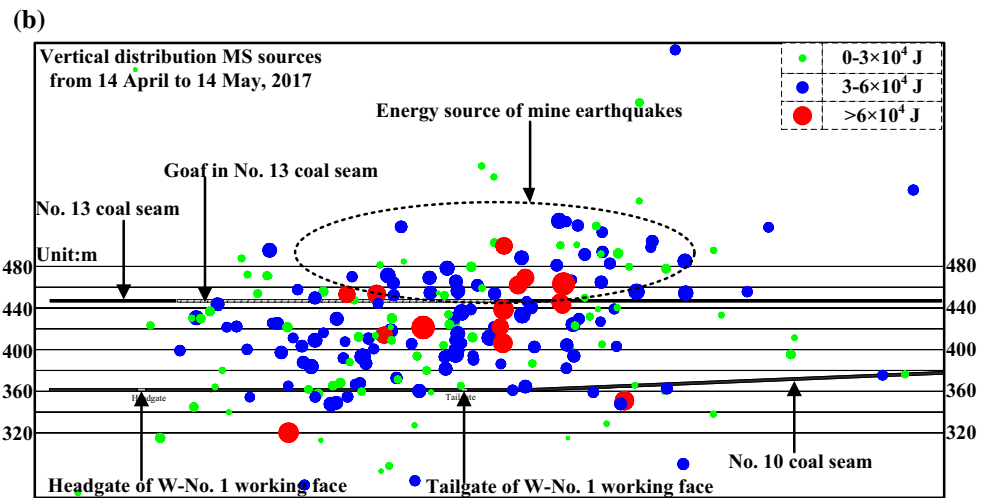
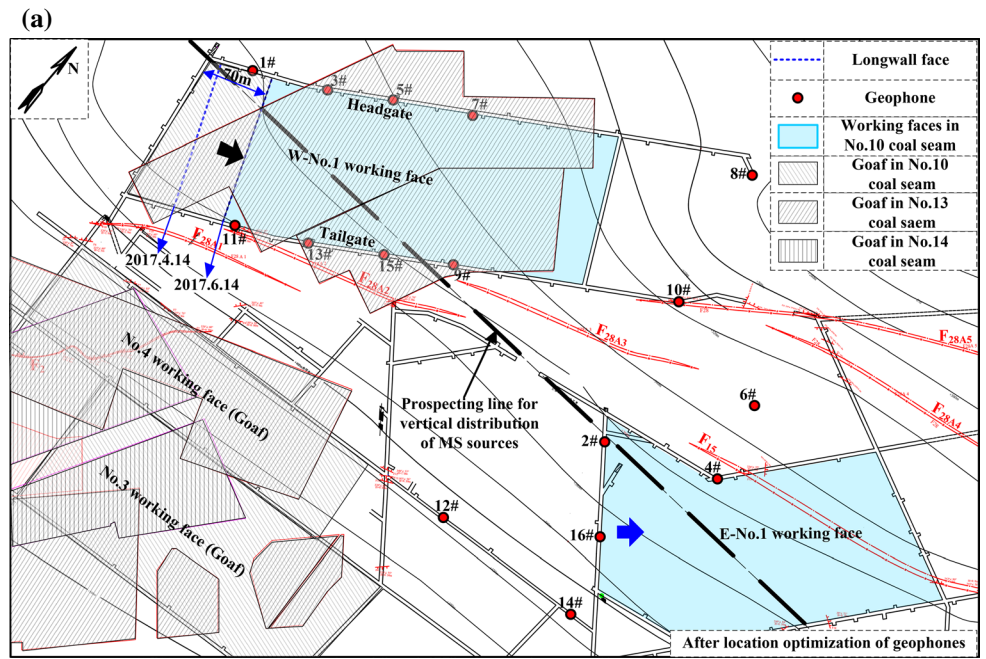
without any mine earthquake or mining disturbance occurring between 18 November 2014 and 17 July 2015, whereas the second six rock bursts were accompanied by mine earthquakes that occurring between 21 October 2015 and 29 February 2016. One common characteristic is that all these rock bursts only created slight damage, even when accompanied by mine earthquakes. The first four bursts obviously belong to the “high in situ stress plus high mining-induced stress plus low disturbance stress” rock burst; for the second six bursts may belong to “high in situ stress plus high mining-induced stress plus high disturbance stress” rock burst.

If this is the case, then where did the mine earthquake come from? There is no doubt that the hard roof fracturing of the No. 10 coal seam could not lead to these rock bursts. The MS monitoring scheme of W-No. 1 working face and monitoring results from 14 April to 14 June 2017 are provided in Fig. 15 (note: the stoping of W-No. 1 working face will last until 2018, and the stoping speed is 1.2 m per day). During this period, the stoping distance of the headgate was only 70 m, but there were nearly thirty mine earthquakes that occurred without any damage in the working face. From Fig. 15b, c, several MS sources are shown to come from the roof of No. 13 coal seam. Especially from 14 April to 14 May, the stoping distance was only 10 m, which means

that the fracturing of the main roof of No. 10 coal seam was impossible. Therefore, it could be concluded that the energy source of the mine earthquakes came from the roof fracturing of No. 13 coal seam. Based on the distance between the energy source and the burst region, the high disturbance stress could be classified into the far-field high disturbance stress, i.e., roof fracturing of No. 13 coal seam, and the near-field high disturbance stress, i.e., roof fracturing of No. 10 coal seam. Therefore, the second six rock bursts that were accompanied by mine earthquakes between 21 October 2015 and 29 February 2016 belong to the “high in situ stress plus high mining-induced stress plus far-field high disturbance stress”, which is illustrated in Fig. 16. Above all, there are two reasons that the MS monitoring results used in discussing the MS sources are reasonable. First, the MS monitoring scheme provided in this paper was optimized once. Second, the emphasis is that find out where the MS sources come from, and the monitoring results could prove this accompanied with the stoping distance of No. 4 working face.

Practical experiences reveal that “high in situ stress plus high mining-induced stress plus low or far-field high disturbance stress” rock burst could be mitigated. The damage of this kind of rock burst was rather slight. The roof fracturing of No. 13 coal seam was just an inducing factor, whereas

Fig. 15 Sketch of MS monitoring scheme of W-No. 1 working face, and monitoring results of vertical distribution of MS sources from 14 April to 14 June, 2017. **a** Monitoring scheme **b** 14 April to 14 May, 2017 **c** 14 May to 14 June, 2017



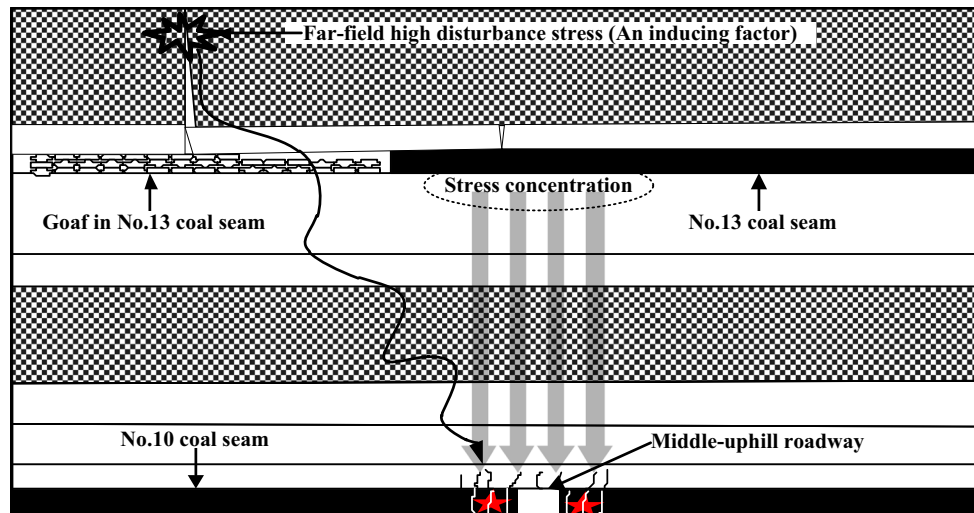


Fig. 16 Sketch of “high in situ stress plus high mining-induced stress plus far-field high disturbance stress” rock burst mechanism

the high stress concentration was the main controlling factor. It could be mitigated or even controlled through the use of a suitable mitigating strategy. For instance, although the middle-uphill roadway experienced a high frequency of rock bursts, there was no burst again after applying large-diameter drilling, water infusion and floor loosening blasting methods.

As illustrated in Fig. 11, a trapezoid area with a high in situ stress plus high mining-induced stress was formed in the No. 4 working face. During the burst occurrence period, the distances from the headgate and tailgate to the middle-uphill roadway were 30–90 m and 101–164 m, respectively. The analysis of this part mainly focuses on the three serious rock bursts, which include the “3.31” event, “4.12” event and “4.19” event. Figure 17 shows the pressure variation law during the stoping process of No. 4 working face from 11 March to 18 April, 2016. Compared with Table 5, it again reveals that the roof fracturing of No. 13 coal seam was an inducing factor, and that the high stress concentration and the main hard roof fracturing of No. 4 working face were the controlling factor. For example, bursts accompanied by mine earthquakes occurring on 30 March, 4 April and 6

April, only caused slight or no damage, whereas bursts that occurred without mine earthquakes on 23 March and 17 April caused slight damage. The mechanisms of the three serious rock bursts are as follows.

As shown in Fig. 17, when one weak rock burst without an accompanying mine earthquake caused slight damage to the tailgate, the abutment pressure varied from 25.8 to 8.2 MPa on 23 March, which indicates the roof fracturing of No. 10 coal seam. Then, two mine earthquakes occurred on 30 March, and one of them induced a weak rock burst. However, a serious rock burst accompanied by mine earthquake occurred on 31 March. During this burst, the pressures of longwall face and tailgate all decreased rapidly from 28.4 to 23.9 MPa, and from 25.2 to 20.5 MPa, respectively. Obviously, the hard roof fracturing of No. 10 coal seam was the main factor. Thus, the “3.31” event belongs to the “high in situ stress plus high mining-induced stress plus near-field high disturbance stress” rock burst. When both the near-field and far-field high disturbance stresses exist, we define the burst as a “high in situ stress plus high mining-induced stress plus near-field high disturbance stress” rock burst because

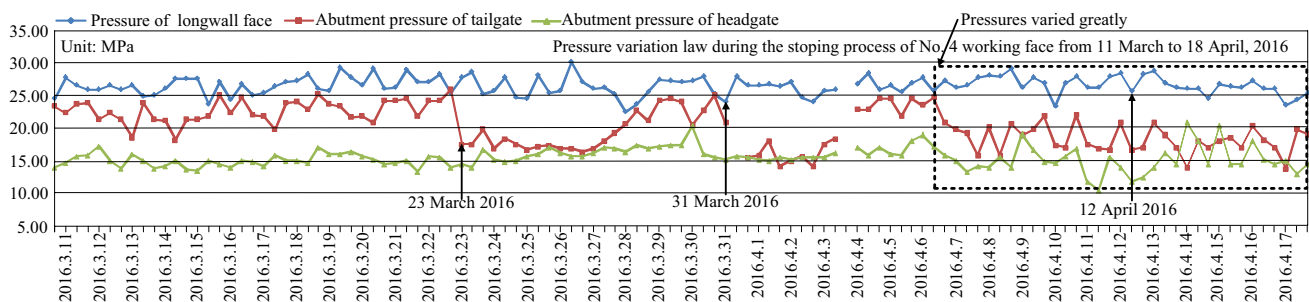


Fig. 17 Pressure variation law during the stoping process of No. 4 working face from 11 March to 18 April, 2016

the far-field high disturbance stress is not the main controlling factor.

The mechanism of “4.12” and “4.19” events was similar to the “3.31” event. As illustrated in Fig. 17, when the “4.12” event occurred, the pressures of longwall face, headgate and tailgate all experienced a sharp decrease. Especially before the “4.19” event, the pressure of No. 4 working face varied greatly, which means that the main hard roof of No. 10 coal seam frequently fractured. Based on the above analysis, it could be concluded that the “4.12” and “4.19” events also belong to the “high in situ stress plus high mining-induced stress plus near-field high disturbance stress” rock burst. The mechanism of this type of rock burst is illustrated in Fig. 18. Although large-diameter drilling and water infusion methods were applied to the No. 4 working face, these two methods could not mitigate the near-field high disturbance stress coming from the main hard roof fracturing of No. 10 coal seam. If the hard roof pre-fracturing method was applied, serious rock bursts might be mitigated.

5.3 A Detailed Classification of Rock Burst Mechanisms

From the point of stress, the occurrence of rock bursts is controlled by three major factors: the in situ stress, mining-induced stress and disturbance stress, which are shown in Fig. 14a. Thus, the stress criterion for rock burst occurrence can be expressed as Eq. (1) (Guo et al. 2017b).

$$\sigma_i + \sigma_m + \sigma_d > [\sigma] \quad (1)$$

where σ_i is the in situ stress, σ_m is the mining-induced stress, σ_d is the disturbance stress, and $[\sigma]$ is the critical stress required for rock burst formation.

Moreover, compared with these new findings and phenomena (i.e., high/low disturbance stresses and far-field/near-field high disturbance stresses) in the above analysis, a more detailed classification system of rock burst mechanisms could be established, which is illustrated in Fig. 19. There are nine types of rock bursts based on the main causes and different disturbance stresses. In this classification, great mining depth and geological structures often lead to high in situ stress; coal pillars, island working faces, goaf, the end stoping process and multi-seam mining lead to high mining-induced stress; blasting, drilling, gates driving, coal cutting and other mining activities generate low disturbance stress; main hard roof fracturing is the source of near-field high disturbance stress; and mine earthquakes and long-distance hard roof fracturing often generate far-field high disturbance stress. The nine types are (1) “high in situ stress plus low disturbance stress” (rock bursts in the side-uphill roadway), (2) “high mining-induced stress plus low disturbance stress”, (3) “high in situ stress plus high mining-induced stress plus low disturbance stress” (four rock bursts occurred between 18 November 2014 and 17 July 2015 in the middle-uphill roadway), (4) “high in situ stress plus far-field high disturbance stress”, (5) “high in situ stress plus near-field high disturbance stress”, (6) “high mining-induced stress plus far-field high disturbance stress”, (7) “high mining-induced stress plus near-field high disturbance stress”, (8) “high in situ stress plus high mining-induced stress plus far-field high disturbance stress” (six rock bursts occurred between 21 October 2015 and 29 February 2016 in the middle-uphill roadway), and (9) “high in situ stress plus high mining-induced stress plus near-field high disturbance stress” (serious rock bursts occurred in the No. 4 working face) rock bursts.

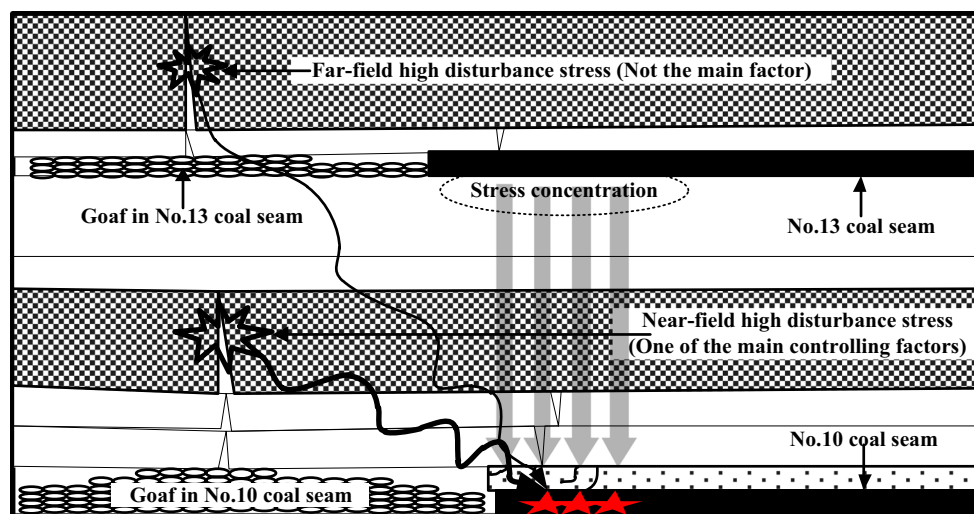
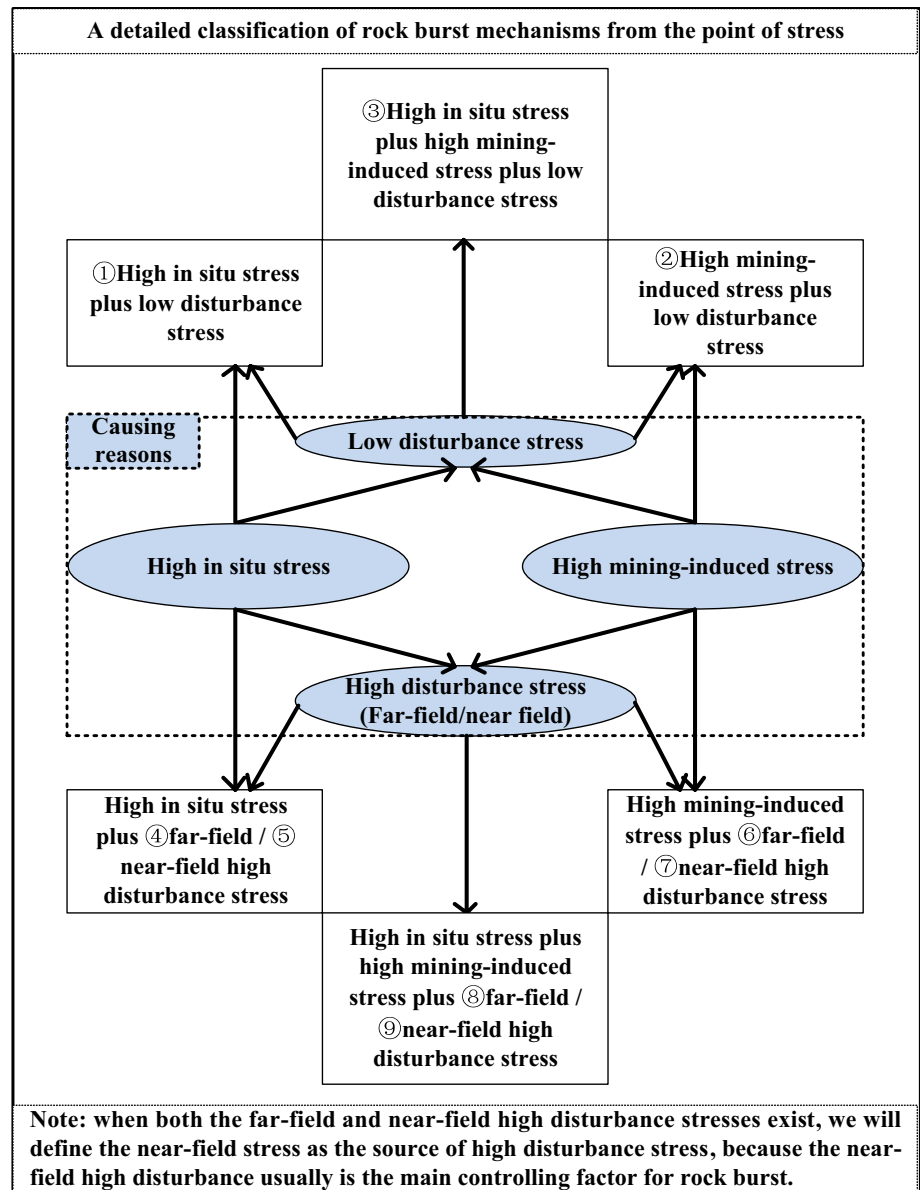


Fig. 18 Sketch of “high in situ stress plus high mining-induced stress plus near-field high disturbance stress” rock burst mechanism

Fig. 19 Sketch of a detailed classification system of rock burst mechanisms



5.4 Mitigation Guidelines

Practical experiences have proven that low disturbance stress and far-field high disturbance stress are difficult to be controlled, but high in situ stress, high mining-induced stress and near-field high disturbance stress can be mitigated. Based on this viewpoint, we provide some guidelines here for mitigating different types of rock burst, as shown in Fig. 20. For rock burst types (1), (2), (3), (4), (6) and (8), they could be mitigated or controlled through two aspects, which consist of mining arrangements and mitigating methods. The mining arrangement includes a reasonable layout of working faces, protective layer mining, etc., and the commonly used mitigating methods consist of destress blasting, water infusion, destress drilling, grooving, etc. (Holub et al. 2011; Konicek et al. 2011, 2013;

Li et al. 2008, 2014; Wang et al. 2012a, b; Su et al. 2014; Díaz Aguado and Gonzalez Nicieza 2007; Guo et al. 2017a). For rock burst types (5), (7) and (9), roof pre-fracturing could be used for mitigating the near-field high disturbance stress, except that these methods are used for mitigating high in situ stress or high mining-induced stress concentration. In addition, when these mitigating strategies or methods are applied, parameter optimization must be completed for consideration of secondary disaster avoidance and cost-effectiveness.

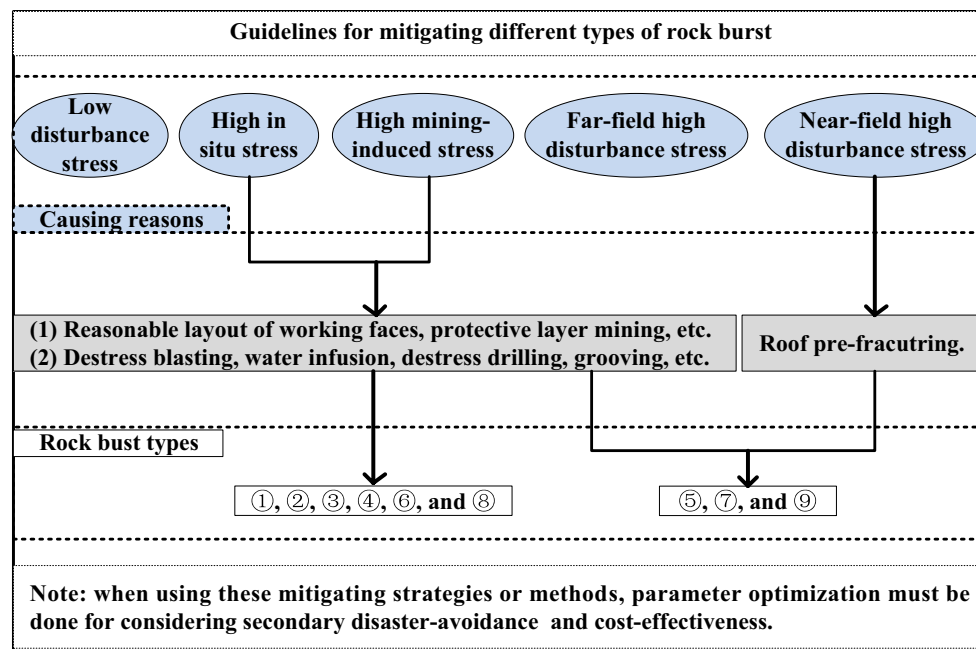


Fig. 20 Guidelines for mitigating different types of rock burst

6 Conclusions

In this paper, we first introduce the engineering geological characteristics of No. 10 coal seam of Da'anshan Coal Mine. Then, we select three typical areas for further research that had experienced a high frequency of rock bursts between October 2014 and April 2016. The temporal and spatial characteristics, geological and mining conditions, and other information related to these bursts have been reviewed in detail. We study the rock burst mechanisms and mitigating strategies based on these bursts. The primary conclusions are as follows:

1. There are twenty-four rock bursts, which were mainly focused in the side-uphill roadway, middle-uphill roadway and No. 4 working face. One new phenomenon appeared: fourteen of the rock bursts occurred in the side-uphill and middle-uphill roadways after 6–16 months of roadway excavation, which means that creep-induced rock bursts account for nearly 54% of the total. Experiences in the No. 10 coal seam reveal that creep-induced rock bursts concentrate in high static stress areas, such as great mining depth, geological structures, coal pillars, etc. They have a close relation to the high in situ/mining-induced stress, and their damage was less serious compared with those bursts that occurred during the stopping process.
2. Two other new phenomena include mine earthquake/long-distance roof fracturing, which may be an inducing factor for rock burst occurrence, and left coal pillars in the upper coal seam, which could lead to high mining-induced stress concentration. Thus, under multi-seam mining conditions, the layout of working faces of upper coal seam must be designed reasonably so as not to bring stress concentration or other difficulties to the underlying coal seam mining.
3. In addition to the inherent property of CBL, the rock burst occurrence is caused by the superposition of in situ stress, mining-induced stress and disturbance stress. Based on these causes, the rock burst mechanism can be classified into three major groups (Fig. 14b). However, the disturbance stress includes low disturbance stress (blasting, drilling, gates driving, coal cutting and other mining activities), near-field high disturbance stress (main hard roof fracturing) and far-field high disturbance stress (mine earthquake and long-distance hard roof fracturing). When considering the different disturbance stresses, there are nine types of rock bursts (Fig. 19).
4. Practical experiences in Da'anshan Coal Mine have proven that low disturbance stress and far-field high disturbance stress are difficult to be controlled, but high in situ stress, high mining-induced stress and near-field high disturbance stress can be mitigated. Therefore, some guidelines for mitigating or controlling different types of rock bursts are provided in this paper (Fig. 20). The parameter optimization of different mitigating strategies must be done for consideration of secondary disaster avoidance and cost-effectiveness before application.

Although the above research provides some valuable conclusions, more research needs to be done. First, the four new phenomena, i.e., creep-induced rock bursts, mine earthquakes, long-distance roof fracturing and left coal pillars in the upper coal seam, are new points of research. Second, the influences of different disturbance stresses on the rock burst occurrences need to be further study, except for the main causes of high in situ stress/high mining-induced stress. Third, this paper only gives the mitigation guidelines without consideration of parameter optimization of different mitigating strategies or methods. Based on rock burst classification and the related mitigation guidelines, we can research the most suitable destressing strategy for each type of rock burst.

Acknowledgements The research described in this paper was financially supported by State Key Research Development Program of China (No. 2016YFC0801401), National Natural Science Foundation of China (No. 51604165, No. 51674160, No. 51474137 and No. 51704181), Shandong Province Natural Science Foundation (No. ZR2016EEB23), Tai'shan Scholar Engineering Construction Fund of Shandong Province of China, Taishan Scholar Talent Team Support Plan for Advantaged & Unique Discipline Areas. The authors thank the peer reviewers and Editors for their valuable comments and suggestions, which have greatly improved the manuscript.

References

- Brauner G (1994) Rockbursts in coal mines and their prevention. A.A. Balkema, Rotterdam
- Cai W, Don LM, He J, Liu HS, Li ZL, Ding YL (2014) Mechanical genesis of Henan (China) Yima thrust nappe structure. *J Cent South Univ* 21:2857–2865
- Cai W, Dou LM, Si GY, Cao AY, He J, Liu S (2016) A principal component analysis/fuzzy comprehensive evaluation model for coal burst liability assessment. *Int J Rock Mech Min Sci* 81:62–69
- Cording EJ, Hashash YMA, Oh J (2015) Analysis of pillar stability of mined gas storage caverns in shale formations. *Eng Geol* 184:71–80
- Corkum AG, Board MP (2016) Numerical analysis of longwall mining layout for a Wyoming Trona mine. *Int J Rock Mech Min Sci* 89:94–108
- Díaz Aguado MB, Gonzalez Nicieza C (2007) Control and prevention of gas outbursts in coal mines, Riosa–Olloniego coalfield, Spain. *Int J Coal Geol* 69:253–266
- Feng Y, Jiang FX, Li JD (2015a) Evaluation method of rock burst hazard induced by overall instability of island coal face. *J China Coal Soc* 40(5):1001–1007 (in Chinese)
- Feng GL, Feng XT, Chen BR, Xiao YX, Yu Y (2015b) A microseismic method for dynamic warning of rockburst development processes in tunnels. *Rock Mech Rock Eng* 48(5):2061–2076
- Feng GL, Feng XT, Chen BR, Xiao YX (2015c) Microseismic sequences associated with rockbursts in the tunnels of the Jinping II hydropower station. *Int J Rock Mech Min Sci*. 80:89–100
- Feng XT, Zhang CQ, Qiu SL, Zhou H, Jiang Q, Li SJ (2016) Dynamic design method for deep hard rock tunnels and its application. *J Rock Mech Geotech Eng* 8:443–461
- GB/T 25217.2-2010 (2010) Classification and laboratory test method on bursting liability of coal. Standards Press of China, Beijing (in Chinese)
- Gu ST, Huang RF, Tan YL, Li WS, Xiao ZM (2015) Formation mechanism of anticline structure and its disastrous mechanism of rock burst. *J Min Saf Eng* 32:59–64 (in Chinese)
- Guo H, Yuan L, Shen BT, Qua QD, Xue JH (2012) Mining-induced strata stress changes, fractures and gas flow dynamics in multi-seam longwall mining. *Int J Rock Mech Min Sci* 54:129–139
- Guo WY, Tan YL, Yang ZL, Zhao TB, Hu SC (2017a) Effect of saturation time on the bursting liability indexes of coal and its application for rock burst mitigation. *Geotech Geol Eng*. <https://doi.org/10.1007/s10706-017-0300-2>
- Guo WY, Zhao TB, Tan YL, Yu FH, Hu SC, Yang FQ (2017b) Progressive mitigation method of rock bursts under complicated geological conditions. *Int J Rock Mech Min Sci* 96:11–22
- Han J, Zhang HW, Lan TW, Li S (2014) Geodynamic environment of rockburst in western Beijing coalfield. *J China Coal Soc* 39:1056–1062 (in Chinese)
- Haramy KY, Kneisley RO (1990) Yield pillars for stress control in longwall mines—case study. *Int J Min Geol Eng* 8:287–304
- He H, Dou LM, Gong SY, Zhou P, Xue ZJ, Jiang H (2011) Study of mining shock in high tectonic stress zones. *J China Univ Min Technol* 40(1):7–13
- He J, Dou LM, Lu CP (2012) Characteristic and prevention research on rock burst of thin coal seam. *J China Coal Soc* 37(7):1094–1098 (in Chinese)
- Holub K, Rušajová J, Holec̃ko J (2011) Particle velocity generated by rockburst during exploitation of the longwall and its impact on the workings. *Int J Rock Mech Min Sci* 48:942–949
- Huang WP, Yuan Q, Tan YL, Wang J, Liu GL, Qu GL, Li C (2017) An innovative support technology employing a concrete-filled steel tubular structure for a 1000-m-deep roadway in a high in situ stress field. *Tunn Undergr Space Technol*. <https://doi.org/10.1016/j.tust.2017.11.007>
- Iannacchione AT, Zelanko JC (1995) Occurrence and remediation of coal mine bursts: a historical review. US Department of the Interior, U.S. Bureau of Mines, Special Publication 01-95, pp 27–68
- Ji F, Lu JF, Shi YC, Zhou CH (2013) Mechanical response of surrounding rock of tunnels constructed with the TBM and drill-blasting method. *Nat Hazards* 66:545–556
- Jiang FX (2006) View point of spatial structures of overlying strata and its application in coal mine. *J Min Saf Eng* 23(1):30–33 (in Chinese)
- Jiang PF, Kang HP, Zhang J, Lin J, Si LP (2011) Mechanism of load-transfer between coal pillars with different widths in mining the short-range seams. *J Min Saf Eng* 28(3):345–349 (in Chinese)
- Jiang YD, Wang HW, Xue S, Zhao YX, Zhu J, Pang XF (2012) Assessment and mitigation of coal bump risk during extraction of an island longwall panel. *Int J Coal Geol* 95:20–33
- Jiang FX, Qu XC, Ni XH, Wang FQ, Tang ZB (2013a) Case study on the mine earthquake caused by hard rock fracture in Baodian Coal Mine. *J China Coal Soc* 38(S2):319–324 (in Chinese)
- Jiang YD, Wang T, Zhao YX, Wang C (2013b) Numerical simulation of fault activation pattern induced by coal extraction. *J China Univ Min Technol* 42(1):1–5 (in Chinese)
- Kaiser PK, Cai M (2012) Design of rock support system under rock-burst condition. *J Rock Mech Geotech Eng* 4(3):215–227
- Kidybinski A (1981) Bursting liability indices of coal. *Int J Rock Mech Min Sci Geomech Abstr* 18:295–304
- Konicek P, Saharan MR, Mitri H (2011) Destress blasting in coal mining -state-of-the-art review. *Procedia Eng* 26:179–194
- Konicek P, Soucek K, Stas L, Singh R (2013) Long-hole destress blasting for rockburst control during deep underground coal mining. *Int J Rock Mech Min Sci* 61:141–153
- Lee SM, Parkb BS, Lee SW (2004) Analysis of rockbursts that have occurred in a waterway tunnel in Korea. *Int J Rock Mech Min Sci* 41(3):1–6

- Li ZH, Dou LM, Lu CP, Mu ZL, Can AY (2008) Study on fault induced rock bursts. *Int J Min Sci Technol* 18:321–326
- Li ZL, Dou LM, Cai W, Wang GF, He J, Gong SY, Ding YL (2014) Investigation and analysis of the rock burst mechanism induced within fault-pillars. *Int J Rock Mech Min Sci* 70(9):192–200
- Li WF, Bai JB, Peng S, Wang XY, Xu Y (2015) Numerical modeling for yield pillar design: a case study. *Rock Mech Rock Eng* 48:305–318
- Li XH, Pan F, Li HZ, Zhao M, Ding LX, Zhang WX (2016) Prediction of rock-burst-threatened areas in an island coal face and its prevention: a case study. *Int J Min Sci Technol* 26:1125–1133
- Lu CP, Liu GJ, Liu Y, Zhang N, Xue JH, Zhang L (2015) Microseismic multi-parameter characteristics of rockburst hazard induced by hard roof fall and high stress concentration. *Int J Rock Mech Min Sci* 76:18–32
- Lu CP, Liu GJ, Zhang N, Zhao TB, Liu Y (2016) Inversion of stress field evolution consisting of static and dynamic stresses by microseismic velocity tomography. *Int J Rock Mech Min Sci* 87:8–22
- Maleki H, Rigby S, McKenzie J, Faddies T (2011) Historic mine designs and operational practices used in deep mines for controlling coal bumps. In: Proceedings of the 45th US rock mechanics/geomechanics symposium. American Rock Mechanics Association, Alexandria, VA, doc ID 11-276
- Meng FZ, Zhou H, Wang ZQ, Zhang LM, Kong L, Li SJ, Zhang CQ (2016) Experimental study on the prediction of rockburst hazards induced by dynamic structural plane shearing in deeply buried hard rock tunnels. *Int J Rock Mech Min Sci* 86:210–223
- Meng FZ, Zhou H, Wang ZQ, Zhang CQ, Li SJ, Zhang LM, Kong L (2017) Characteristics of asperity damage and its influence on the shear behavior of granite joints. *Roc Mech Rock Eng*. <https://doi.org/10.1007/s00603-017-1315-y>
- Ning JG, Wang J, Tan YL, Zhang LS, Bu TT (2017a) In situ investigations into mining-induced overburden failures in close multiple-seam longwall mining: a case study. *Geomech Eng* 12(4):657–673
- Ning JG, Wang J, Jiang JQ, Hu SC, Jiang LS, Liu XS (2017b) Estimation of crack initiation and propagation thresholds of confined brittle coal specimens based on energy dissipation theory. *Rock Mech Rock Eng*. <https://doi.org/10.1007/s00603-017-1317-9>
- Peng SS (2008) Coal mine ground control. Department of Mining Engineering/College of Engineering and Mineral Resources, Morgantown
- Qu QD, Xu JL, Wu RL, Qin W, Hu GZ (2015) Three-zone characterisation of coupled strata and gas behaviour in multi-seam mining. *Int J Rock Mech Min Sci* 78:91–98
- Sainoki A, Mitri HS (2014) Dynamic behaviour of mining-induced fault slip. *Int J Rock Mech Min Sci* 66:19–29
- Sainoki A, Mitri HS (2016) Dynamic modelling of fault slip induced by stress waves due to stope production blasts. *Rock Mech Rock Eng* 49:1–17
- Si GY, Jamnikar S, Lazar J, Shi JQ, Durucan S, Korre A, Završek S (2015) Monitoring and modelling of gas dynamics in multi-level longwall top coal caving of ultra-thick coal seams, Part I: Borehole measurements and a conceptual model for gas emission zones. *Int J Coal Geol* 144–145:98–110
- Singh SP (1988) Burst energy release index. *Rock Mech Rock Eng* 21:149–155
- Singh AK, Singh R, Maiti J, Kumar R, Mandal PK (2011) Assessment of mining induced stress development over coal pillars during depillaring. *Int J Rock Mech Min Sci* 48:805–818
- Su CD, Zhai XX, Wei XZ, Li BF (2014) Influence of saturation period on bursting liability indices for coal seam 2# in Qianqiu Coal Mine. *Chin J Rock Mech Eng* 33(2):235–242 (in Chinese)
- Suchowerska AM, Merifield RS, Carter JP (2013) Vertical stress changes in multi-seam mining under supercritical longwall panels. *Int J Rock Mech Min Sci* 61:306–320
- Sun ZW (2003) Numerical simulation on stress field distribution in partial transformation area of coal seam. *Ground Press Strata Contr* 20:95–100 (in Chinese)
- Tan YL (1990) The relation between geotectonic stress and impact ground pressure in Mentougou mine. *J Shandong Min Inst* 9(3):264–267 (in Chinese)
- Tan YL, Zhang Z, Zhao TB (2011) AE pattern of rock burst disaster induced by strata activation in coal mine. *Disaster Adv* 4(4):29–33
- Tan YL, Yu FH, Ning JG, Zhao TB (2015) Design and construction of entry retaining wall along a gob side under hard roof stratum. *Int J Rock Mech Min Sci* 77:115–121
- Tan YL, Guo WY, Gu QH, Zhao TB, Yu FH, Hu SC, Yin YC (2016) Research on the rockburst tendency and AE characteristics of inhomogeneous coal-rock combination bodies. *Shock Vib* 2:1–11
- Tan YL, Liu XS, Ning JG, Lv YW (2017) In situ investigations on failure evolution of overlying strata induced by mining multiple coal seams. *Geotech Test J* 40(2):1–14
- Wang XN, Huang RQ (1998) Analysis of deformation and failure features characteristics of rock under unloading conditions and their effects on rock burst. *J Mt Res* 16:281–285 (in Chinese)
- Wang SB, Zhang X (2008) Relation between geological structures and in situ stresses in underground coalmines. *J China Coal Soc* 33:738–742 (in Chinese)
- Wang CW, Jiang FX, Liu JH (2012a) Analysis on control action of geologic structure on rock burst and typical cases. *J China Coal Soc* 37(S2):263–268 (in Chinese)
- Wang JM, Zeng XH, Zhou JF (2012b) Practices on rockburst prevention and control in headrace tunnels of Jinping II hydropower station. *J Rock Mech Geotech Eng* 4(3):258–268
- Wang HW, Jiang YD, Xue S, Pang XF, Lin ZN, Deng DX (2017) Investigation of intrinsic and external factors contributing to the occurrence of coal bumps in the mining area of western Beijing. *China Rock Mech Rock Eng* 50(4):1033–1047
- Whyatt JK, Varley F (2009) Regional bumps: case studies from the 1958 bump symposium. *Trans Soc Min Metall Explor* 326:101–105
- Xie YM, Li TB (2004) Primary discussion on blast's affection on rock burst. *Chin J Geol Hazard Contr* 15:61–64 (in Chinese)
- Yan P, Zhao Z, Lu W, Fan Y, Chen XR, Shan ZG (2015) Mitigation of rock burst events by blasting techniques during deep-tunnel excavation. *Eng Geol* 188:126–136
- Yu B, Zhang ZY, Kuang TJ, Liu JR (2016) Stress changes and deformation monitoring of longwall coal pillars located in weak ground. *Rock Mech Rock Eng* 49(8):1–13
- Zhai C, Xiang XW, Xu JZ, Wu SL (2016) The characteristics and main influencing factors affecting coal and gas outbursts in Chinese Pingdingshan mining region. *Nat Hazards* 82(1):507–530
- Zhang Z (2015) Research of stress distribution and stability of roadways' surrounding rock with typical geological variation in coal mine. PhD thesis, Shandong University of Science and Technology, Qingdao (in Chinese)
- Zhang CQ, Feng XT, Zhou H, Qiu SL, Wu WP (2012) Case histories of four extremely intense rockbursts in deep tunnels. *Rock Mech Rock Eng* 45:275–288
- Zhang JF, Jiang FX, Zhu ST, Zhao L (2016) Width design for gobs and isolated coal pillars based on overall burst-instability prevention in coal mines. *J Rock Mech Geotech Eng* 8(4):551–558
- Zhang GC, Liang SJ, Tan YL, Xie FX (2018) Numerical modeling for longwall pillar design: a case study from a typical longwall panel in China. *J Geophys Eng*. 15(1):121–134
- Zhao YX, Jiang YD, Wang T, Gao F, Xie ST (2012) Features of microseismic events and precursors of rock burst in underground coal mining with hard roof. *J China Coal Soc* 37(12):1960–1966 (in Chinese)
- Zhao TB, Guo WY, Tan YL, Zhang Z, Cheng KK (2016) Research on the mechanics mechanism of rock burst for mining in the variable

- region of coal thickness. *J China Coal Soc* 41(7):1659–1666 (**in Chinese**)
- Zhao TB, Guo WY, Tan YL, Yu FH, Huang B, Zhang LS (2017a) Failure mechanism of layer-crack rock models with different vertical fissure geometric configurations under uniaxial compression. *Adv Mech Eng* 9(11):1–15
- Zhao TB, Guo WY, Tan YL, Lu CP, Wang CW (2017b) Case histories of rock bursts under complicated geological conditions. *Bull Eng Geol Environ*. <https://doi.org/10.1007/s10064-017-1014-7>
- Zhou H, Meng FZ, Zhang CQ, Hu DW, Yang FJ, Lu JJ (2015) Analysis of rockburst mechanism induced by structural plane in deep tunnels. *Bull Eng Geol Environ* 74(4):1435–1451